Certified that the work presented in this thesis is the original work of Mr Radhey Shyam Kaushal carried out under my supervision

Y R Waghmare
Assistant Professor of Physics

Department of Physics
Indian Institute of Technology
Kanpur, India

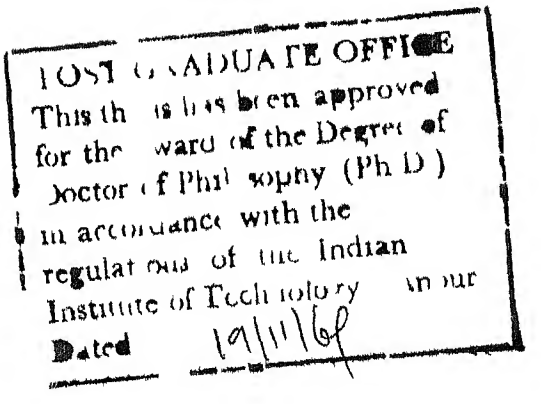

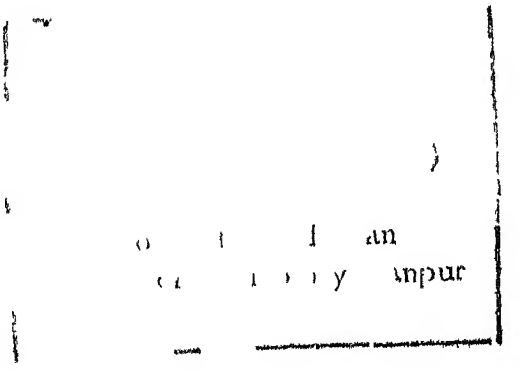

ACKNOWLEDGEMENTS

It is a great pleasure to express my indebtness to Dr Y R Waghmare for his valuable suggestions, keen interest and constant help in all phases of the present work I am thankful to Professor J Mahanty, Head of the Physics Department, I.I T Kanpur for his interest and encouragement I am grateful to Dr G K. Mehta, Dr R M Singru, Dr V i Deshpande and Dr P K Patnaik for many stimulating discussions and suggestions

Thanks are also due to my friends M/s K P Joshi, M C Jain, S K Bose, A K Bhargawa and K P. Singh and to my colleague sisters Meera Murthy and I Kakkar for valuable conversations and their help in preparing the manuscript I wish to thank Dr D K Sood and Mr and Mrs Tiwari for computational help

A major part of my thanks is due to my colleague and friend Mr. P Singh whose close association made my stay at I.I.T.K as pleasent as it could have ever been I am also thankful to Mr R D Tripathi for his immense patience in typing the thesis. Finally, I thankfully acknowledge the financial help of Council of Scientific and Industrial Research, New Delhi, India during the course of this work

TABLE OF CONTENTS

LIST OF TABLES

LIST OF FIGURES

SYNOPSIS

In the present work, our main efforts have been to study the charge distributions and wave functions for light nuclei ($A \leq 16$) which are obtained from Hartree-Fock (HF) calculations with realistic nucleon-nucleon interaction

This thesis consists of four chapters. Chapter I gives a breif summary of information which one gets about the nucleus using various elementary particles as nuclear probes. In Chapter II, by means of high energy electron scattering the charge distributions of ^{4}He, ^{8}Be, ^{12}C and ^{16}O nuclei are studied. For these nuclei, the HF charge distributions and the calculated form factors are compared with electron scattering data as well as with other theoretical results. In case of ^{4}He, the agreement of the calculated form factor with recent experiments of Frosch et al is found to be much better than the results of other authors with modified oscillator charge density for short range dynamical correlations. However, the agreement with experiments for ^{12}C and ^{16}O is somewhat poor. A simple model, derived from the Gaussian form, is also used for ^{4}He charge distribution. As compared to the results of some of the authors, this simple model gives somewhat better results. Further, we establish a relationship between the parameters of two conventional models (harmonic

oscillator and Fermi) used for the charge distribution of a given nucleus in the small momentum transfer limit. In this chapter we also discuss the effects of short range repulsive correlations in the charge density.

Chapter III describes the two nucleon emission process following the π^--capture in complex nuclei as a tool to test the nuclear HF wave functions We derive a general expression for the absorption rate in the HF representation. The results obtained are used for the study of π^-- capture in ^{12}C nucleus. The calculated angular distributions of the absorption rate and the branching ratios are in fairly good agreement with the available experimental data. We also compare these results with the results obtained by various other approaches which have been used to introduce the effect of short range correlations in the wave function of pion-capturing pair of nucleons. Our results are found to be better in some cases. Calculations are also done with harmonic oscillator wave functions. In this case we study the corrections due to various effects, in particular those arising from (i) short range dynamical correlations, (ii) final state nucleon-nucleus scattering and (iii) final state nucleon-nucleon scattering to the absorption rate. It is found that the results obtained with pure harmonic oscillator model are in reasonably good agreement with experiments. However, the correction due to the first effect increases the absorption

rate whereas the corrections due to last two effects suppress the absorption for back-to-back emission (where the pion-capture rates dominate) of the nucleon pair. The effect of these corrections on the branching ratio R (= $W(pn \rightarrow nn)/W(pp \rightarrow pn)$) is studied in great detail We further compare and discuss these two nuclear (Hartree-Fock and harmonic oscillator) models in the light of pion-capture results

Finally, in Chapter IV the scattering of high energy muons on spin $-\frac{1}{2}$ light nuclei ($A < 4$) is studied by using generalized Rosenbluth formula The contribution of the non-negligible muon mass to the Rosenbluth scattering is found to be important at relatively low energies and large momentum transfers. Further, we compare the calculated muon-proton scattering results with the experiments at the incident muon momentum of 2 5 BeV/c, where the contribution of the mass term is small. At such high energies the possibility of obtaining information about muon structure from muon-proton scattering is pointed out. Predictions of the muon scattering on ^3H and ^3He are also made and the results are compared with the available electron scattering data at relatively small values of momentum transfer.

CHAPTER I

INTRODUCTION

In recent years the use of elementary particles has become an important tool for studying nuclear structure physics This is primarily because of the fact that nucleons take part in a large number of basic processes The use of nucleons and photons to investigate the nature of nuclear forces and various other nuclear properties such as spin, parities, excitation of nuclear energy levels, transition probabilities etc has already been known for a long time A reasonable success is also achieved by using other elementary particles such as electrons, muons, π-mesons, K-mesons, Λ particles etc as nuclear probes The scattering as well as capture of these particles by nuclei is a valuable source of information regarding the nuclear structure Here, we shall briefly summarize the pieces of information which have been obtained about the nucleus by means of these processes

The interest in the study of such high energy processes may be for three reasons (i) to investigate the nucleus itself, or (ii) to obtain information on the interaction of elementary particles with nucleons and/or (iii) to know about the projectile itself

By bombarding elementary particles on nuclei not much can probably be known about the projectile This is

for two reasons firstly, the exact nature of nuclear forces is not known, secondly, the inaccuracies involved in the measurement of nuclear size by other means, may be comparable to that of the size of the projectile. For the known projectile-nucleus interaction, however, the nucleon or a few nucleon system target whose size is somewhat accurately known, can be helpful to some extent in this respect Recently, some such attempts[1] have been made to extract the pion form factor from $\pi^{\pm}$-^{4}He scattering In these attempts, one essentially, eliminates the charge symmetric strong interaction of pion with the nucleus by comparing the scattering cross sections for π^+ and π^- on ^{4}He The remaining electromagnetic scattering would then provide the information regarding the pion form factor Another example of this case is the muon-proton scattering which we shall discuss in Chapter IV in detail

By bombarding elementary particles on nuclei, somewhat more information can be extracted on the interaction of the projectile with nucleons A specific example of this is the study of hypernuclei which is a source of information concerning the weak and strong interactions of hyperons with nucleons High energy processes can provide a Λ particle (the lightest hyperon) which may be absorbed in a nucleus The fact that Λ particle is distinguishable from nucleons and is not hindered by the Pauli principle from occupying any of the levels in that nucleus, can reveal the most characteristic features of hypernuclei In a single particle

picture of the nucleus, the core of (A-1) nucleons acts as the source of an average potential for the Λ The shape of this potential is determined by the nuclear density distribution and the Λ-N interaction It is the problem of hypernuclear spectroscopy to relate the properties of hypernuclei to the basic interactions and to reveal the nature of the latter In the last few years such studies have been made for a large number of nuclei[2] It is found that the Λ-nuclear interactions although strong, are relatively weaker than the N-N interaction After the much improved low energy Λ-p scattering data have become available[3] the difference between Λ-nuclear interactions in hypernuclei and the free Λ-N interaction has become of particular interest

The nonmesonic decays of Λ-hypernuclei leads to new information on the weak decay interactions of the Λ-hyperon One such decay is

$$(\Lambda + N) \longrightarrow N + N$$

which is effective only for Λ particles in the presence of nucleons. There is no satisfactory evidence so far for leptonic decays of hypernuclei

Thus, the main interest at present is in the study of nuclei using some known form of the projectile-nucleus interaction. Further, the nature of this interaction is responsible to some extent for the types of information which one gets about the nucleus If this interaction is

electromagnetic, the electromanetic properties of nuclei e g charge and current distributions, electromagnetic transitions etc can be studied On the other hand, one can learn about the nature of nuclear forces, nuclear density etc by using strongly interacting projectiles It should be noted that, while one is looking for the properties which arise due to strong interactions, the effects due to electromagnetic interaction can either be neglected or a correction be made for them, since latter is much weaker ($\sim 1/137$) than the former

Before coming to the particles of interest for the present work, mention may be made of K-mesons (kaons) The use of kaons in probing the structure of complex nuclei is mainly attributed to K-mesic atoms The study of such atoms can give the information about correlations among nucleons For instance, a kaon interacting with a nucleon leads to a reaction

$$K + N \longrightarrow Y + \pi$$

If, however, another nucleon is available in the vicinity, the reaction may follow in a nonpionic pattern

$$K + N + N \longrightarrow Y + N$$

The relative yield of nonpionic to pionic K-absorption in nuclei provides a measure of two-nucleon correlations in nuclei From the experimental point of view, the data available[4] from nuclear emulsion techniques are less accurate and insufficient in order to study the nuclear correlations However, these experiments show that about 20% of all K-absorption at rest goes through this nonpionic multinucleon

capture Theoretically, somewhat stronger nature of K-N interaction gives rise to the complexity of reaction mechanism

The study of K-mesic atoms can also throw some light on the nuclear surface[5] This is due to the fact that the nature of kaon-nucleus interaction allows the absorption from orbits of high n-values Since, the nuclear density in the extreme tail region is affected by the presence of strongly interacting kaons, which again complicates the process, the study of nuclear surface from K-mesic atoms still remains an open question

In this work we shall confine ourselves to the study of a few nuclear processes involving electrons, muons and π-mesons (pions) Though, a detailed survey of earlier work on these processes is given in the respective chapters, a few more relevant points can be mentioned here for the sake of completeness

During the last fifteen years, the scattering of high energy electrons (elastic as well as inelastic) by nucleons and nuclei has been extensively studied[18-27] It has been the most successful method of investigating the structure of such targets This is because of the fact that electron-nucleus interaction is purely electromagnetic and is well studied compared to other known interactions Further, the electron beams of sufficiently high energy are now available For the elastic scattering, the electrostatic interaction strongly dominates so that it becomes possible

to learn about the distribution of protons in the nucleus Details of this point will be discussed in the next chapter The sensitivity of proton distribution is governed by the de Broglie wave length of the incident electron of energy E, which is given by

$$\lambda = \frac{197.2}{E(MeV)} F \qquad (1F = 10^{-13} \text{ cm})$$

Thus, in order to become sensitive to structural details one must use electrons of several hundred of MeV

The study of muonic atoms also gives information on the distribution of nuclear charge Negative muons, which get stopped in matter are captured in atomic orbits and as a result of successive transitions the emission of muonic X-rays takes place. Because of the larger muon mass (compared to the electron mass) these X-rays are about 200 times more energetic (and orbits are smaller by the same factor) than the corresponding electronic case Thus, muon gets a chance to 'observe' the nuclear size The measurement[6] of $3D \rightarrow 2P$ and $2P \rightarrow 1S$ spectra provide sufficient information to determine parameters of nuclear charge distribution (see section (2 3)) for spherical as well as for deformed heavy nuclei In case of light nuclei, the probability of penetration of muon into the nucleus, even in 1S orbit, is small Therefore, such measurements can tell more about the distribution of nuclear charge in the surface region rather than in the central region

The choice of muon as a high energy projectile on nucleons and nuclei is as useful as electron for revealing the structure of such targets[7] In addition to the fact that more intense muon beams from pion decay have now become available, muon offers several advantages over electron Firstly, they come naturally polarized Secondly, because of larger muon mass compared to electron the radiative corrections become negligibly small The philosophy of recent studies on muon scattering is to compare the results with corresponding electron scattering measurements at high momentum transfers in order to detect possible structure effects which would distinguish the scattering particles. No significant difference between the electron and muon scatterings on nuclei has been found experimentally, at a given value of momentum transfer[7] However, the scattering of muon by proton for large values of momentum transfer can reveal this difference We shall discuss this point in detail in Chapter IV

The excitation of nuclear energy levels by the inelastic scattering of electrons from complex nuclei provides a convenient means of studying dynamical aspects of nuclear structure[8] By means of this process one can study the properties of excited states of nuclei, in particular their spins, parities, and the strength and structure of the transition operators connecting the ground and excited states This is also a powerful tool for the study of two-body and higher order correlations among nucleons inside nuclei These

correlations are related to the variations of local charge density in the neighbourhood of a particular proton in the nucleus Further, these correlations are conditioned by the Pauli principle, finite size of nuclei and the two-particle interaction between the nucleons Such correlations have been the subject of study for the last several years[9] Only in recent years[34-37] from the analysis of elastic electron scattering data for large momentum transfers, it has become possible to learn about the short-range dynamical correlations in nuclei

Finally, mention may be made of pion as a probe of nuclear structure In recent years, the scattering as well as absorption processes of pion by nuclei have achieved somewhat greater success in comparison to the processes involving other strongly interacting particles[10]. This is because of the fact that pion has several advantages over other elementary particles In comparison with a nucleon few points can be noted (i) Pion is a boson of spin zero and just like photon it can disappear in the final state of the reaction; (ii) it can exist in three charge states π^+, π^0, π^-, (iii) the pion mass is about 1/7 of the nucleon mass, which causes smaller recoil corrections. These three points make the kinematics somewhat simpler (iv) The relation of π-nuclear interaction with π-N interaction seems to be easily understandable than the corresponding relation for the nucleon All these points make the pion-nuclear processes calculable to a better approximation than the processes induced by the nucleon

Another advantage of pion is the fact that the π-N interaction up to kinetic energies of the order of 300 MeV is much better understood than the N-N interaction[90] At energies smaller compared to (3,3) resonance energy (~ 200 MeV laboratory energy) the s-wave interaction is important In this region, the elastic scattering of pions gives the information about π-nuclear optical potential and the distribution of nucleons in the nucleus Since π-N interaction is rather weak at low energies, the impulse approximation may be used Thus, a multiple scattering calculation provides a good description of very low-energy π-nuclear interaction[11] However, the validity of this approximation is questionable in the resonance region

Studies of charge - exchange reactions of pions such as single charge exchange ${}^{A}_{Z}X(\pi^{\mp}, \pi^{0})_{Z\mp1}{}^{A}Y$ and double charge-exchange ${}^{A}_{Z}X(\pi^{\mp}, \pi^{\pm})_{Z\mp2}{}^{A}Y$, can also provide information on nuclear structure For single charge-exchange reactions not much is known experimentally Double charge-exchange reactions are of interest mainly for two reasons (i) One can produce the isobaric analogue states corresponding to $\Delta T_z = \pm 2$ and (ii) one can learn about the short range two-nucleon correlations in nuclei[12] Unfortunately, the cross sections obtained for this reaction are too small.

It is well known that the real pion absorption in nuclei possibly occurs (i) at zero or low energies (free absorption) and (ii) even at negative energies (bound orbits) A detailed study of the absorption of very low energy ($\lesssim$ 30 MeV)

pions is made by Ericson and Ericson[11] on the basis of multiple scattering theory. This approach is useful for dealing with overall absorption features such as widths and shifts of the levels of π-mesic atoms. Recently, experimental[13] as well as theoretical[14] attempts have been made to study the single nucleon states in nuclei by means of free pion absorption followed by single-nucleon emission. However, these attempts are still insufficient to provide further details of the nucleus. For free pion absorption the energy of the positive pion is somewhat larger but well below the resonance energy. The study of the absorption of bound pion is attributed to π-mesic atoms. A negative pion of several MeV energy brought to rest in matter is quickly bound in a low lying mesonic orbit by the Coulomb field of the nucleus. In these orbits (particularly in 1S and 2P), the pion is very close to the nucleus and the strong Yukawa interaction ($\pi^- + p \rightarrow n$) quickly annhilates it.

In order to conserve energy and momentum, the absorption of bound pions takes place by a nucleon in a correlated nucleon-pair. This is because once the pion at rest is captured by the nucleus, it releases 139.6 MeV energy (the pion rest mass) in the nucleus. If this much energy is given to a resting nucleon in the nucleus then that nucleon should come out with a momentum of about 525 MeV/c. However, since the Fermi momentum is only about 250 MeV/c, the one-nucleon-process is strongly suppressed. As a consequence the dominant pion capture involves at least two

nucleons in the process The relative momentum, which is one-half the difference of the acquired momenta of the nucleons in the pion-capturing (p c) pair is thus about 360 MeV/c It would correspond to a relative distance of about 0 5 F (to be more accurate, it should be noted that some of the energy is needed to overcome the binding of the nucleons, and the kinetic energy of each emitted nucleon is only about 50 MeV which leads to a relative distance of about 0 67 F) On the other hand, the range of repulsive core of the nuclear force is of the same order Thus, the short-range nuclear correlations would affect the pion capture in the nucleus

In the case of bound pion absorption, if one of the nucleons of the p c pair strongly scattered by the other nucleons loses too much of its kinetic energy to be emitted, then a 'one-nucleon emission process' would occur More than two nucleon emission process is also possible if either the p c pair of nucleons knock out some nucleons or the nucleus excited by them evaporates some nucleons However, there are now several experimental evidences[57-60] which verify the emission of two-nucleons following the π^--capture The nonradiative and nonmesonic two-nucleon emission process is sometimes referred to as 'nucleonic capture'. In Chapter III we shall study this process in considerable detail Lastly, mention should be made of radiative capture of stopped pion in complex nuclei. This process, dynamically related to muon-capture, has recently yielded valuable

information for the nucleus From the measurement of high energy γ-ray spectrum (cf $\pi^- + p \rightarrow n + \gamma$) it is found that this process amounts to 1-3% of the total capture rate[15] This ratio which is weakly dependent on the mass number A, is fairly well explained by Delorme and Ericson[16] in terms of the impulse approximation and the Fermi gas model

From the above survey following points can be noted (i) The two-nucleon correlation problem in nuclei may be attacked through quite different means such as K^--capture, elastic and inelastic high energy electron scattering, double charge-exchange scattering of pions and π^--capture (ii) Among the processes involving kaons and pions, the nucleonic capture of pion seems to be a very reliable method at present for the study of these correlation effects in light nuclei In particular, our discussions will be focussed on the Hartree-Fock theory which is used in other nuclear structure calculations In Chapter II, starting with Hartree-Fock charge distribution we study various other models of nuclear charge distribution in the light of presently available elastic electron scattering data for light nuclei ($A \leq 16$) Here we also discuss the effects of correlations in nuclear charge density

In Chapter III, we study the process of nucleonic capture of pions in complex nuclei, such as ^{12}C, as a tool for testing the nuclear Hartree-Fock wave functions In this chapter we also study various effects, in particular

those arising from (i) short-range dynamical correlations, (ii) final state nucleon-nucleon interaction, and (iii) final state nucleon-nucleus interaction on the absorption rate Finally, in Chapter IV, we study the scattering of high energy muons on proton and trinucleon systems (^{3}H and ^{3}He) The effects of non-negligible muon mass (compared to electron mass in electron scattering) in the scattering cross section are studied in this chapter

CHAPTER II

CHARGE DISTRIBUTION IN LIGHT NUCLEI AND HIGH ENERGY ELECTRON SCATTERING

2.1 Introduction

The elastic scattering of high energy electrons by nuclei is a source of most accurate and detailed information about the charge distributions in nuclei. Theoretically, the scattering from a point nucleus was first investigated by Mott[17] and later on, the effects due to finite nuclear size were studied by several authors. A systematic and extensive experimental study of such finite size effects has been carried out by Hofstadter[18,19] and his collaborators[21-23]. Since excellent reviews[18,19] and books[20] are now available on the subject, we shall not go into the details of earlier work. The experiments on p-shell nuclei were performed by Meyer-Berkhout et al[22] with improved and higher energies. They have analysed their data by using various functional forms of nuclear charge distribution such as uniform, oscillator, exponential, Fermi etc. Crannell[23] and others[24] have studied nuclei in the intermediate ($A \geqslant 40$) and heavy mass regions ($A > 160$). Recently, more improved data have been obtained for light[25,26] as well as for heavy[27] nuclei.

The end product of the elastically scattered electrons by an extended nucleus of charge Ze is a differential cross section. For relativistic electrons, in the first Born approximation it is given by

$$\frac{d\sigma}{d\Omega} = \left(\frac{Ze^2}{2E}\right)^2 \frac{\cos^2 \theta/2}{\eta \sin^4 \theta/2} \left|F(q)\right|^2 \qquad (2\ 1)$$

where θ is the (laboratory) scattering angle and q is the 3-momentum transfer given by[+]

$$q = (2E/\eta) \sin \theta/2 \qquad (2\ 2)$$

where E is the energy of the incident electron (assumed to be very large compared to the electron mass) η is the recoil correction factor for the nucleus and it is equal to $(1 + (2E/M_T) \sin^2 \theta/2)^{\frac{1}{2}}$ In case when M_T, the mass of the nucleus, is very large $\eta \simeq 1$ In eqn (2 1) the quantity F(q), the so-called nuclear 'form factor' or 'structure factor' , is given by

$$F(q) = \int \rho(\vec{r})\, e^{i \vec{q} \cdot \vec{r}}\, d^3r \qquad (2\ 3)$$

i e F(q) is the Fourier transform of $\rho(r)$, the nuclear charge density which is normalized such that

$$\int \rho(\vec{r})\, d^3r = 1 \qquad (2\ 4)$$

Alternatively, the quantity $\left|F(q)\right|^2$ is defined as the ratio of the experimental cross section to the point charge cross section

From the angular distribution of elastically scattered electrons, an important property of the nucleus

---

[+]We shall be using natural units $\hbar = c = 1$ throughout this chapter

which one extracts is the charge distribution $\rho(\vec{r})$ For spherically symmetric charge distribution, eqn (2 3) can be written as

$$F(q) = (4\pi/q) \int_0^\infty \rho(r)\, r \sin(qr)\, dr \qquad (2\ 5)$$

Another quantity which we come across very often along with the charge distribution is the root mean square (rms) charge radius The mean square radius (the second moment of the distribution) is defined as

$$\langle r^2 \rangle = \int \rho(\vec{r})\, r^2\, d^3r \qquad (2\ 6)$$

Only in past few years[28], it has become possible for spin non-zero nuclei that by measuring the cross section for elastic electron scattering at 180°, the information about the magnetic structure of nuclei can be obtained The choice of a scattering angle of 180° comes from arguments based on time-reversal invariance and parity conservation It is shown by Pratt, Walecka and Griffy[28] that only odd magnetic multipole moments contribute to the elastic scattering cross section However, in this work we shall be dealing all the time with spin zero nuclei where the question of magnetic scattering does not arise

In studying the nuclear structure problems by means of high energy electrons many theoretical models for the distribution of charge have been suggested As such it is difficult to correlate the parameters obtained in such different distributions However, experimentally it is

possible to distinguish between the different proposed types of charge distributions. The distributions that are most commonly used to fit the experimental data are (i) Fermi distribution (Woods-Saxon type) and (ii) harmonic oscillator distribution. The detailed structure of these distributions will be described in sections (2.3) and (2.4). The Fermi distribution gives satisfactory results for medium and heavy nuclei. On the other hand, the validity of oscillator distribution is restricted only to light nuclei. Another distribution which was first used by Helm[29] for medium mass nuclei is the 'folded' distribution. However, the results obtained for this distribution are found to be indistinguishable from those obtained from Fermi distribution. For the use of other distributions we refer to the excellent reviews[18-22].

Recently, Bethe and Elton[30] have proposed another charge distribution which is originally obtained by Bethe[31] in the extension of Thomas-Fermi theory for nuclei. The form of this distribution is

$$\rho_B(r) = \rho_0 [1-\exp((r-R_2)/a_2)]^2 \qquad (2.7)$$

where R_2 and a_2 are parameters. This distribution (like Fermi distribution) is not symmetrical about the half charge density radius. However, it coincides with the Fermi distribution in region of steepest slope (the region where $d\rho(r)/dr$ has largest value) and near $r = R_2$. So far, this form of the distribution has been used only for a few heavy nuclei e.g

^{197}Au It is also used for ^{208}Pb after a little modification The form (2 7) takes somewhat larger values at the centre of the nucleus and gives smaller rms radius compared to the Fermi distribution Perhaps, for light nuclei this form can be used after improving it for the exponential tail

Thus, the main emphasis in analysing results on high energy electron scattering still lies on Fermi and oscillator distributions In order to use them for deformed nuclei they must be modified for the quadrupole as well as for other collective deformations.

The choice of the best $\rho(r)$ is closely related with the choice of nuclear wave functions (particularly with the proton wave functions, if we neglect the finite size of the proton) Thus, the better the approximation of proton wave functions in a nucleus, the better will be the charge distribution The nuclear wave functions are further derivable from the nature of nuclear forces In other words, the results of electron scattering put a check on the theories dealing with the fundamental nucleon-nucleon correlations in nuclei Kulkarni and Swamy[32] have used the charge density obtained from Brueckner's K-matrix theory[33] and they have compared the results with those obtained from electron scattering for ^{40}Ca nucleus. However, the agreement with experiments is poor Perhaps, this discrepancy arises from the marked nonlocality of the potential which Brueckner et al[33] have determined The effect of this nonlocality is also evident in the charge distribution.

Frosch et al[25] have observed the failure of the oscillator model for ^{4}He nucleus at large values of momentum transfer In order to explain these results several attempts[34,35] have been made by modifying the oscillator distribution for short-range repulsive correlations Further calculations based on similar lines, have been done for a few nuclei such as ^{40}Ca, ^{12}C and ^{6}Li by other authors[36,37] In these attempts the correlations were treated in the Jastrow[38] approach, in which the normalization of the states becomes very complicated because the basis loses the property of orthonormality on the application of the correlation operator In the present calculations, therefore, a unitary-model-operator approach[39], which has recently been suggested by Shakin and Waghmare is employed. What they essentially do is to derive an effective interaction starting from a realistic nucleon-nucleon interaction We discuss this approach in detail in section (2 2) The Hartree-Fock theory along with this effective interaction provides satisfactory results for the closed shell nuclei[40,41] This is because of the fact that it provides wave functions which are calculated in a self consistent manner Further calculations have been done[42] for ^{4}He, ^{8}Be, ^{12}C and ^{16}O nuclei In these calculations we have included the corrections due to Coulumb effects and centre of mass motion in a self consistent manner These nuclei satisfy the conditions of spherical Hartree-Fock (except for ^{8}Be) i e. in the shell model picture their occupied and unoccupied orbits are well separated and the concept of sharp Fermi sea is valid In this work we desire

to study the charge densities obtained from the Hartree-Fock (HF) theory In the next section we give the HF charge distributions for the above mentioned nuclei along with a brief description of the theory In section (2 3) these charge distributions are compared with the observed results of electron scattering and also with other models of charge distribution proposed for each nucleus

Further, in section (2 4) attempts are made to correlate the parameters of the Fermi and oscillator distributions in the limit of small momentum transfer. The charge distributions obtained from various theories are compared (particularly for ^{4}He) in section (2 5) In this section we also suggest a simple model for ^{4}He nucleus In section (2 6) we discuss our results based on the comparison between calculated and experimental observations (sections (2 3) and(2 5)) for various nuclei

2 2 Hartree-Fock Charge Distribution

In solving the nuclear structure problems one always comes across the method of approximations This is because of the fact that nucleus is a many body system and the exact nature of nuclear forces is still unknown The Hartree-Fock (HF) method, which has recently been used in nuclear structure studies, is based on the method of successive approximations For the sake of completeness and later on, to have somewhat meaningful discussion of the results we shall briefly review the HF theory used in the present calculations. The details

can be found in references[39-42] In later part of this section we shall only concentrate on the charge distributions obtained from HF theory and for other properties of the nuclei considered we refer to reference[42]

The unitary transformation[44] which gives an effective interaction $\tilde{H}$ from a nucleon-nucleon interaction is given by[39,40]

$$\tilde{H} = e^{iS} H e^{-iS}$$
$$= \sum_{n_1 n_2} t_{n_1 n_2} a^{\dagger}_{n_1} a_{n_2} + \tfrac{1}{2} \sum_{n_1 n_2 n_3 n_4} a^{\dagger}_{n_1} a^{\dagger}_{n_2} \langle n_1 n_2 | e^{iS} \quad X$$
$$X \ (t_1 + t_2 + U_1 + U_2 + V_{12}) \ e^{-iS} - (t_1 + t_2 + U_1 + U_2) X$$
$$X \quad |n_3 n_4\rangle \ a_{n_4} a_{n_3} + \qquad (2.8)$$

where t is the kinetic energy operator and V_{12} is the nucleon-nucleon interaction which may or may not be singular For V_{12}, the Yale potential[45] in which a hard core is assumed, is used The potentials U_1 and U_2 are used to generate single particle nuclear wave functions. In order to simplify the calculations, the form of U_i $(i = 1,2)$ is taken to be the harmonic oscillator potential i e $U_i = \frac{1}{2} k r_i^2$ The operator S is assumed to induce central short-range two-body correlations in the two particle wave functions as

$$e^{iS} \Phi_{n_1 n_2} = \Psi_{n_1 n_2} \qquad (2.9)$$

where Φ's are the unperturbed and Ψ's are the correlated wave functions respectively occurring in expression (2.8)

For some states of the Yale potential it is necessary to use a pseudopotential (a square well type) VP, in order to separate the long range and short range parts of the nucleon-nucleon interaction In that case the interaction potential can be written as,

$$V_{12} = (v^s_{12} + VP) + (v^\ell_{12} - VP) \qquad (2\ 10)$$

The separation of V_{12} into these two parts is then achieved by solving the following two equations,

$$\left.\begin{aligned} &(t_1+t_2+U_1+U_2+v^s_{12}+VP)\,\Psi_{n_1n_2} = (\varepsilon_{n_1}+\varepsilon_{n_2})\,\Psi_{n_1n_2} \\ \text{and}\quad &(t_1+t_2+U_1+U_2)\,\Phi_{n_1n_2} = (\varepsilon_{n_1}+\varepsilon_{n_2})\,\Phi_{n_1n_2} \end{aligned}\right\} (2\ 11)$$

Using eqns (2 8), (2 9) and (2 11) we obtain the effective interaction as,

$$\tilde{H} = \sum_{n_1n_2} \langle n_1 | t | n_2 \rangle\, a^+_{n_1} a_{n_2} + \frac{1}{2} \sum_{n_1n_2n_3n_4} a^+_{n_1} a^+_{n_2} a_{n_4} a_{n_3} \langle \Psi_{n_1n_2} | (v^\ell_{12} - VP + v^{OD}_T) | \Psi_{n_3n_4} \rangle \qquad (2\ 12)$$

wherein the diagonal terms of the tensor force V_T are included in the central part v^ℓ_{12} leaving only the off-diagonal terms v^{OD}_T to be determined However, the second order terms in v^{OD}_T contribute considerably to the nuclear binding and so do the second order terms in the pseudopotential VP These, therefore, must be included in (2 12) Thus, the general two-body effective interaction becomes,

$$\tilde{H} = \sum_{n_1 n_2} \langle n_1 | t | n_2 \rangle \, a^{\dagger}_{n_1} a_{n_2} + \frac{1}{2} \sum_{n_1 n_2 n_3 n_4} a^{\dagger}_{n_1} a^{\dagger}_{n_2} a_{n_4} a_{n_3} \langle \Psi_{n_1 n_2} | \times$$

$$\times \quad [(v^{\ell}_{12} - VP) + v^{OD}_{T} + v^{OD}_{T} \frac{Q}{e} v^{OD}_{T} + VP \frac{Q}{e} VP] | \Psi_{n_3 n_4} \rangle \tag{2 13}$$

where Q is the Pauli operator and e is the appropriate energy denominator. The matrix elements for the Yale potential, by using expression (2 13) are evaluated by Shakin et al[41] for various states of relative angular momentum

In the HF method along with the effective interaction (2 13), finally, one is left with the following equations[43] which are to be solved,

$$\langle \alpha | t | \beta \rangle + \langle \alpha | U | \beta \rangle = \varepsilon_{\alpha} \, \delta_{\alpha\beta} \tag{2 14}$$

where the HF potential U is defined as,

$$\langle \alpha | U | \beta \rangle = \sum_{\gamma=1}^{A} [\langle \alpha\gamma | v_{eff} | \beta\gamma \rangle - \langle \alpha\gamma | v_{eff} | \gamma\beta \rangle] \tag{2 15}$$

Here $\langle v_{eff} \rangle$ is the potential energy term in the expansion (2 13) The correlated basis functions are expanded in terms of the harmonic oscillator functions as,

$$\Psi_{\alpha}(r) = \sum_{n} c^{\alpha}_{n} \, \varphi_{n}(r) \tag{2 16}$$

where c^{α}_{n} are expansion coefficients sometimes called as 'mixing coefficients' Substitution of (2.16) in (2.14) yields

$$\sum_{n'} [\langle n|t|n\rangle + \langle n|U|\bar{n}\rangle] c^{\alpha}_{n'} = \varepsilon_{\alpha} c^{\alpha}_{n} \qquad (2\ 17)$$

where $\langle n|U|n\rangle = \sum_{\mu\mu'} [\langle n\mu|v_{eff}|n\mu'\rangle - \langle n\mu|v_{eff}|\mu' n\rangle] \rho_{\mu\mu'}$

with the probability density (density matrix)

$$\rho_{\mu\mu'} = \sum_{\gamma=1}^{A} c^{\gamma}_{\mu} c^{\gamma}_{\mu'} \qquad (2\ 18)$$

where sum over γ runs over occupied states only If we restrict ourself only upto proton orbitals and correct the coefficients c's (which are to be determined in a self consistent manner) for the Coulumb force then, $\rho_{\mu\mu}$ from (2 18) will give the charge density (now on denoted as HF charge density)

We further assume spherical nuclei Then the single particle states have good angular momentum, and c^{α}_{n} are diagonal in ℓ, j and independent of m (the z-projection of $\vec{j}$) Thus, using c's which are determined in a self consistent manner, the correlated single particle wave functions ψ's from (2 16) can be calculated for proton as well as for neutron orbitals

The HF charge distributions obtained from above calculations are shown in Fig (2 1) for light nuclei such as ^{4}He, ^{8}Be, ^{12}C and ^{16}O They are very much similar to those obtained from the electron scattering experiments[19,25] except that they have a long tail. In case of ^{16}O, a central depression of charge density is also observed in HF results

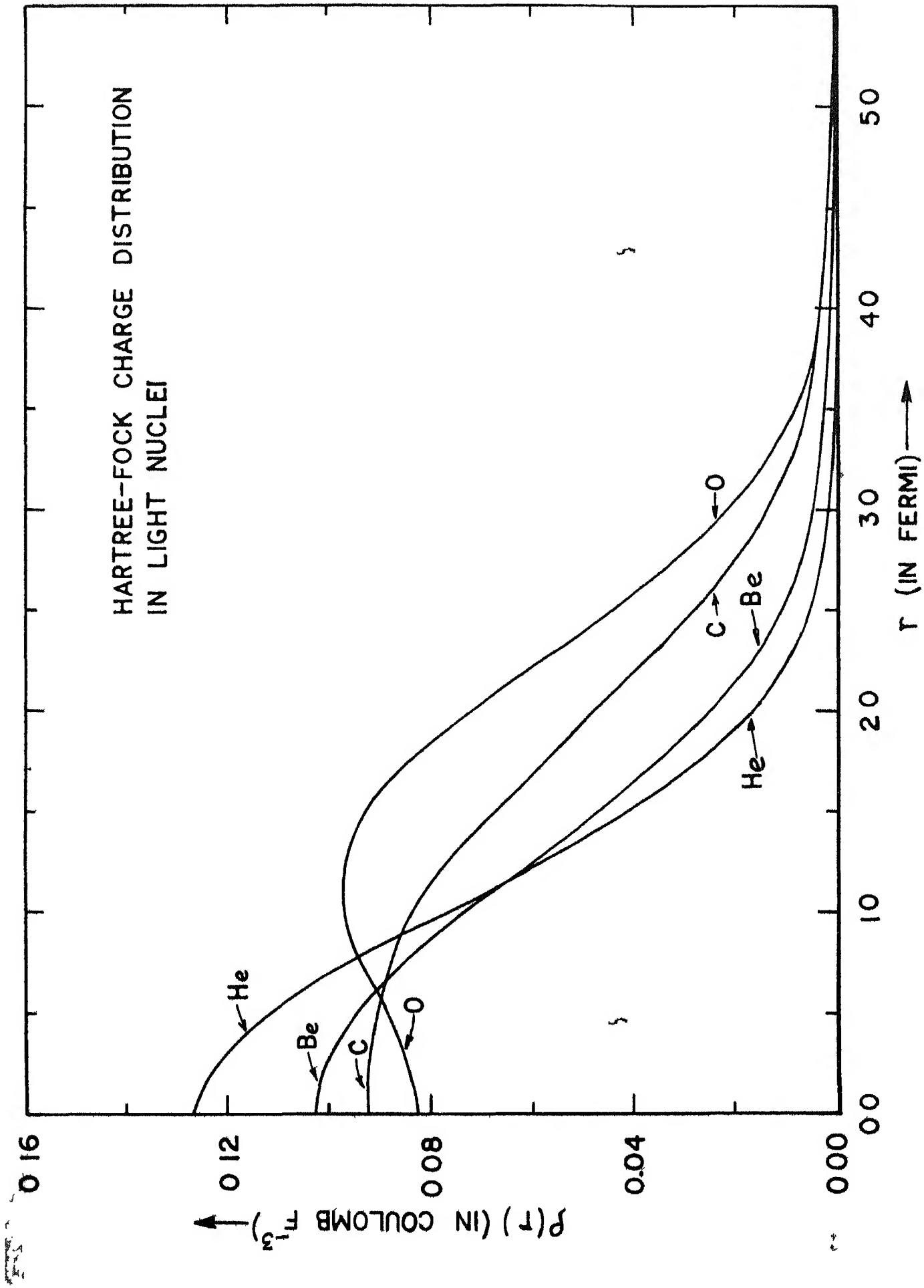
HARTREE-FOCK CHARGE DISTRIBUTION
IN LIGHT NUCLEI
ρ(r) (IN COULOMB F⁻³)
r (IN FERMI)
0.16
0.12
0.08
0.04
0.00
0
10
20
30
40
50
He
Be
C
O
He
Be
C
O

FIG 21

For ^{4}He the HF charge distribution is compared with the results of Tang and Herndon[34] in Fig (2 2) They have modified the ^{4}He wave functions for the short-range nucleon-nucleon forces It is clear from Fig (2 2) that the HF results are in somewhat better agreement with experiments compared to the results of Tang and Herndon[34] for r_c = 0 6 F, where r_c is the hard-core radius (see section (2 5)) The HF results for ^{16}O, are compared in Fig (2 3) with the results obtained from the Brueckner's K-matrix[33] theory The Brueckner-charge-density for ^{16}O falls somewhat faster with r compared to the HF charge density and is mostly accumulated near the centre of the nucleus

In the next section we compare HF results with the experimental results of electron scattering

2 3 Comparison with the Results of Electron Scattering

The success of a theory dealing with nuclear wave functions also depends on how far it can reproduce the results of high energy electron scattering. This is because the form factor F(q) (the Fourier transform of charge density) is directly related to the scattering cross section (cf eqn (2 1)) Although the form factor F(q) in eqn (2 5) have been integrated numerically, in order to know the equivalent parameters for HF distributions we have fitted them with standard models For this purpose, the HF charge distributions for ^{4}He, ^{8}Be and ^{12}C are fitted with the two-parameter Fermi model

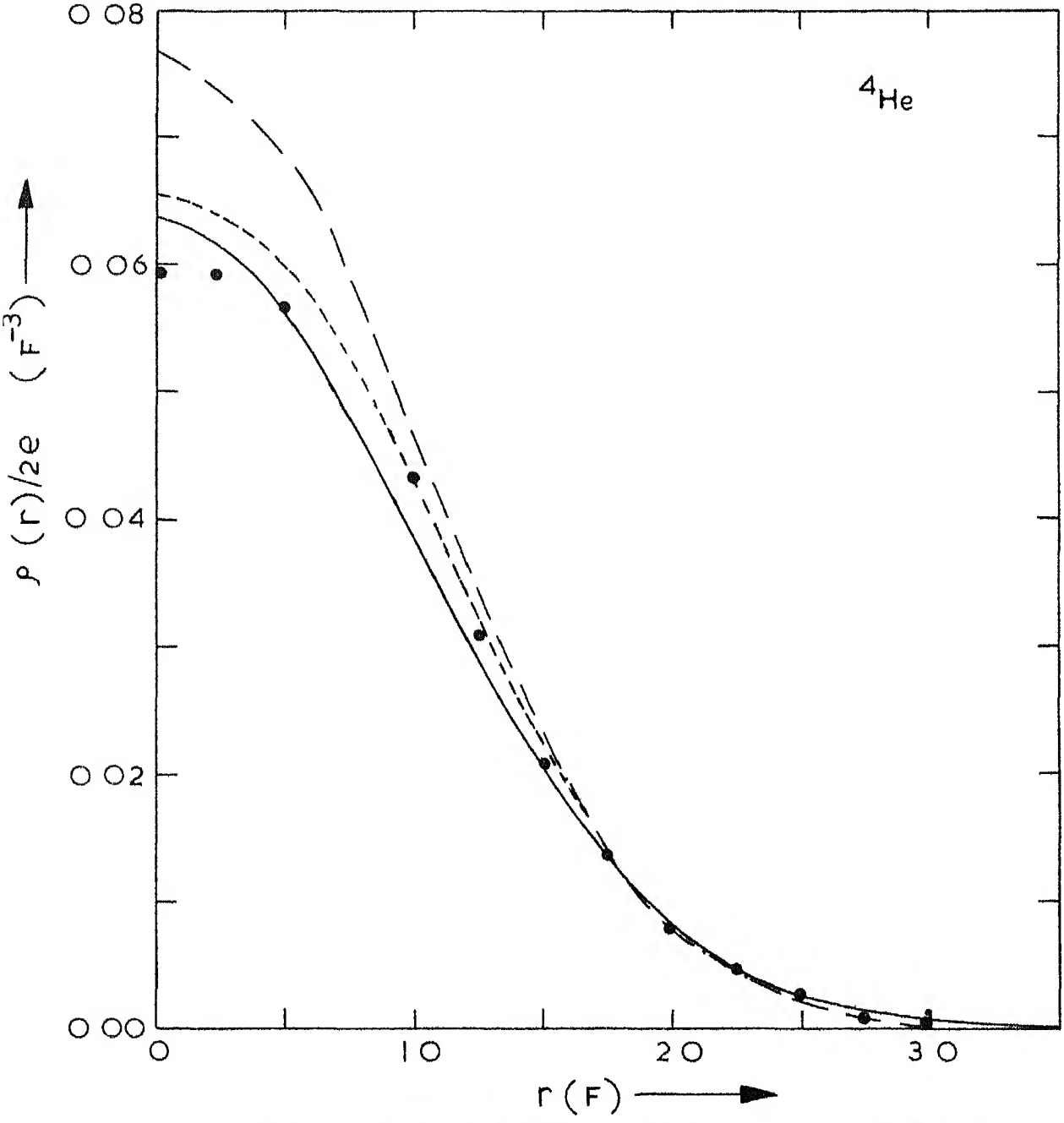

FIG 2 2 Comparison of charge densities for ^{4}He The solid line shows the HF results the dashed and dot-dashed lines show the results of Tang and Herndon (ref. 34) corresponding to r_c = 0 6 F and r_c = 0, 5 F respectively Experimental points are from Frosch et al (ref 25).

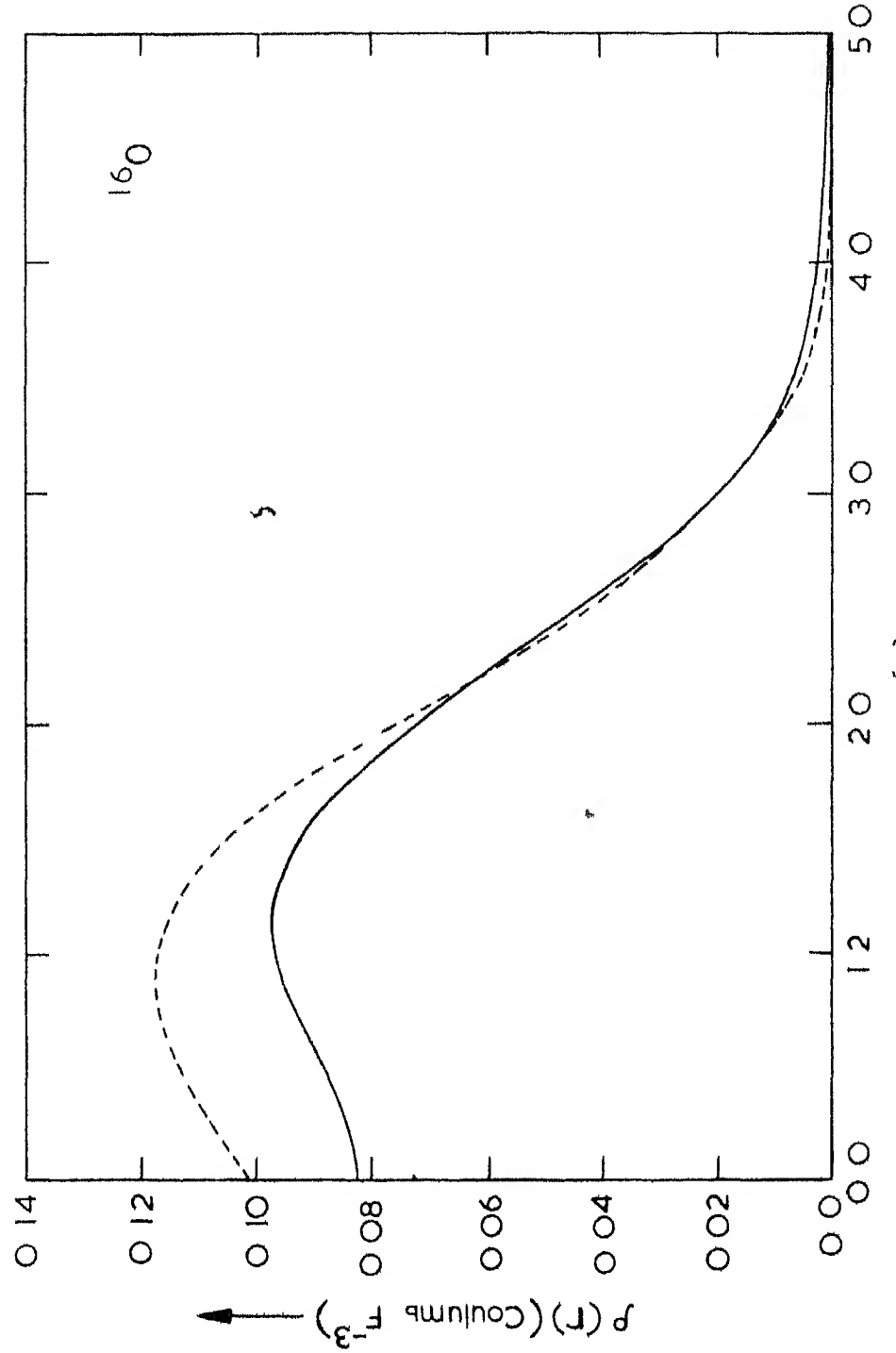

FIG 2 3 **Comparison of charge densities for ^{16}O The solid curve represents the results of HF theory and the dashed curve represents those obtained from Brueckner theory (ref 33)**

$$\rho(r) = \rho_0 \left[1 + \exp((r-c)/a_0)\right]^{-1} \qquad (2\ 19)$$

where c is the half charge density radius (defined as the distance from the centre of the nucleus to a point, where the density reduces to half of the value at the centre) and a_0 is a parameter related to the skin thickness t (the distance over which the density decreases from 90% to 10% of it's maximum value) by the relation $t = 4\ 4\ a_0$ The three-parameter Fermi model,

$$\rho(r) = \rho_1(1+wr^2/c^2) \left[1+\exp((r-c)/a_1)\right]^{-1} \qquad (2\ 20)$$

is used to fit the charge distribution of ^{16}O, where w is a measure of the central depression of charge density In the model (2 20), there is no simple relation between t and a_1 as is the case with model (2 19) Like the earlier results of electron scattering[18,19] from p-shell nuclei, we have not used the oscillator model which is given as

$$\rho(r) = 2\ \pi^{-3/2}\ b^{-3}(2+3\alpha)^{-1}\ (1+\alpha r^2/b^2)\ \exp(-r^2/b^2) \qquad (2\ 21)$$

where b is the oscillator parameter and $\alpha = (Z - 2)/3$ This is due to the fact that it does not have a long tail while the HF charge distribution does have a long tail (see also section (2 2)) The values of the parameters obtained by fitting the two distributions (2 19) and (2 20) to the HF results are compared in Table (II 1) with those obtained by fitting the two distributions directly to the experiments (for all the four nuclei) Using the results of reference(49)

TABLE II-1

The values of equivalent parameters (of Fermi model) obtained for HF charge distribution

Nucleus		$\sqrt{\langle r^2 \rangle}$(F)	c(F)	t(F)	other parameters
^{4}He	HF calculations	1 77	1 18	1 76	-
	Experimental[e]	1 67	1 32	1 45	-
	other authors[a]				-
^{8}Be	HF calculations	3 47	1 42	2 20	-
	Experimental(^{9}Be)	2 50[f]	1 80[g]	2 00[g]	-
^{12}C	HF calculations	2 85	2 10	2.33	-
	Experimental[b]	2 54	2 24	2 20	-
^{16}O	HF calculations[+]	2 58	2 55	1 78	c_1=2 16 F, a_1=0 4 F, w=0 68
	Experimental[c]	2.64	2.60	1.90	
	other authors[d]	2 41	2 35	1 70	

a See Table (II 2)

b Meyer-Berkhout et al (ref 22)

c Hofstadter (ref 19)

d Brueckner et al (ref 33)

e Frosch et al (ref 25)

f Bernheim et al (ref 26)

g. Elton (ref 20)

+ The definition of c_1 is similar to that of c, but their values differ because of the asymmetry of the skin at r = c in the HF charge distribution

for the integral with Fermi distribution, the form factor F(q) and the scattering cross section ($d\sigma/d\Omega$) are calculated analytically for these nuclei by using eqns (2 5) and (2 1) respectively

Recent experiments[25] at large values of momentum transfer indicate clearly a deviation from the Gaussian model for ^{4}He and show a diffraction minimum at $q^2 = 10\ F^{-2}$ The calculated form factor F(q) is shown in Fig (2 4) along with the experimental results of Frosch et al[25] The results of Czyz and Lesniak[34] who have calculated the charge form factor with the lowest order correction to the uncorrelated ground state density are also shown in this figure From this figure it can be noticed that though the agreement of our results with experiments is almost as good as that of Czyz and Lesniak, it is better than that of Tang and Herndon[34] who have made estimation with the Jastrow correlation length of 0 6 F

No experimental information on the charge distribution of ^{8}Be is available[47] As shown in Table (II.1), the HF results predict the rms radius as 3.47 F and half charge density radius c = 1 42 F for ^{8}Be The scattering cross sections at E = 420 MeV are shown in Fig (2 5) from $\theta = 32^\circ$ to 82° The HF results predict a diffraction minimum at $\theta = 80^\circ$ for ^{8}Be Further, in Fig (2 6) the predicted results for ^{8}Be, are compared with the experimental scattering cross sections on ^{9}Be at E = 300 MeV The results are in satisfactory agreement Thus, the correlations

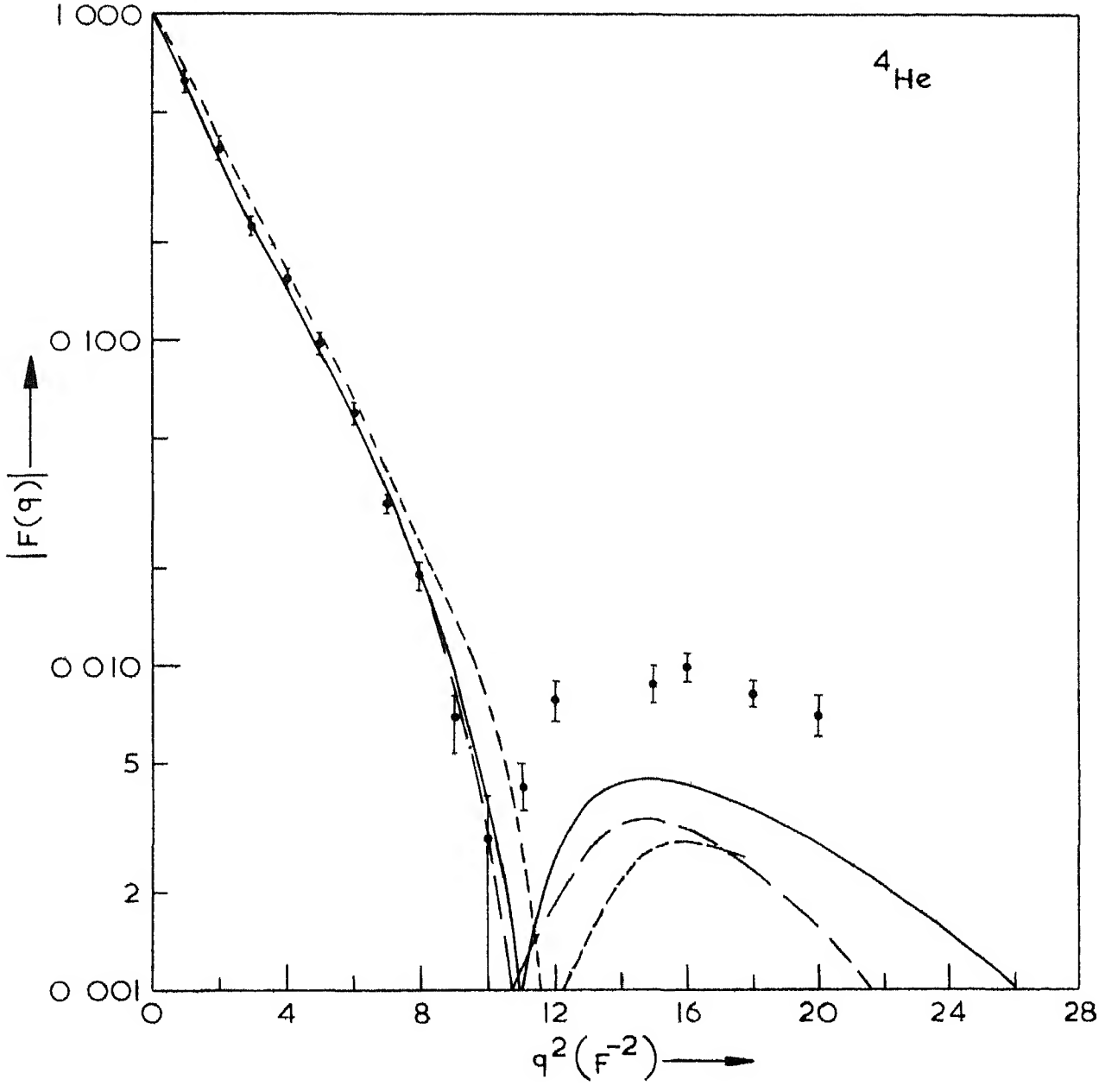

FIG 2 4 Form factor for ^{4}He The solid curve represents the HF results, the dashed curve represents the results of Tang and Herndon (ref 34) for r_c = 0.6 F, and the dot-dashed curve represents the reshlts of Czyz and Lesniak (ref 34) Experimental points of Frosch et al (ref 25) are shown with errors.

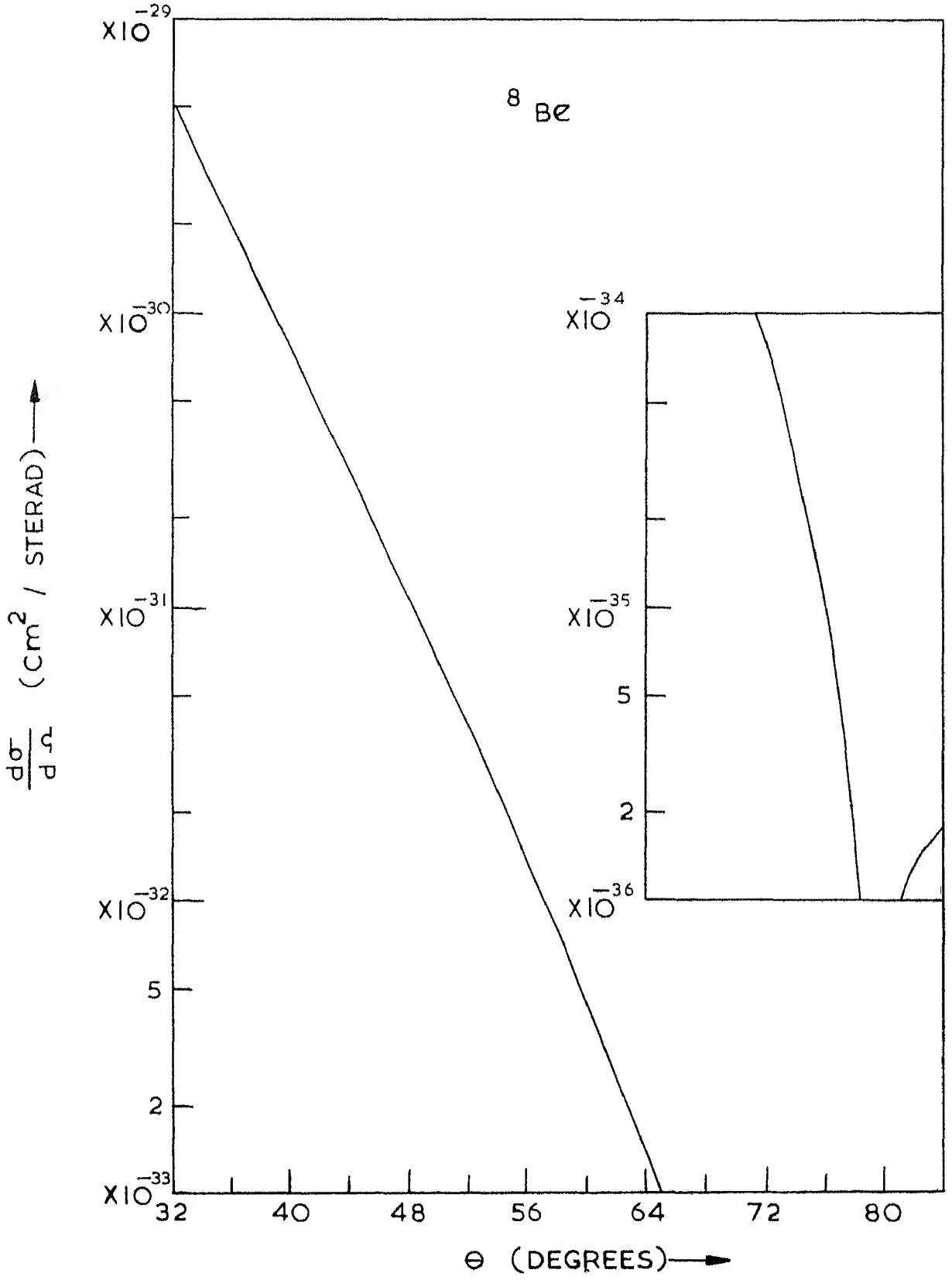

FIG 2 5 **Electron scattering cross sections by ^{8}Be at E = 420 MeV calculated with the HF charge density**

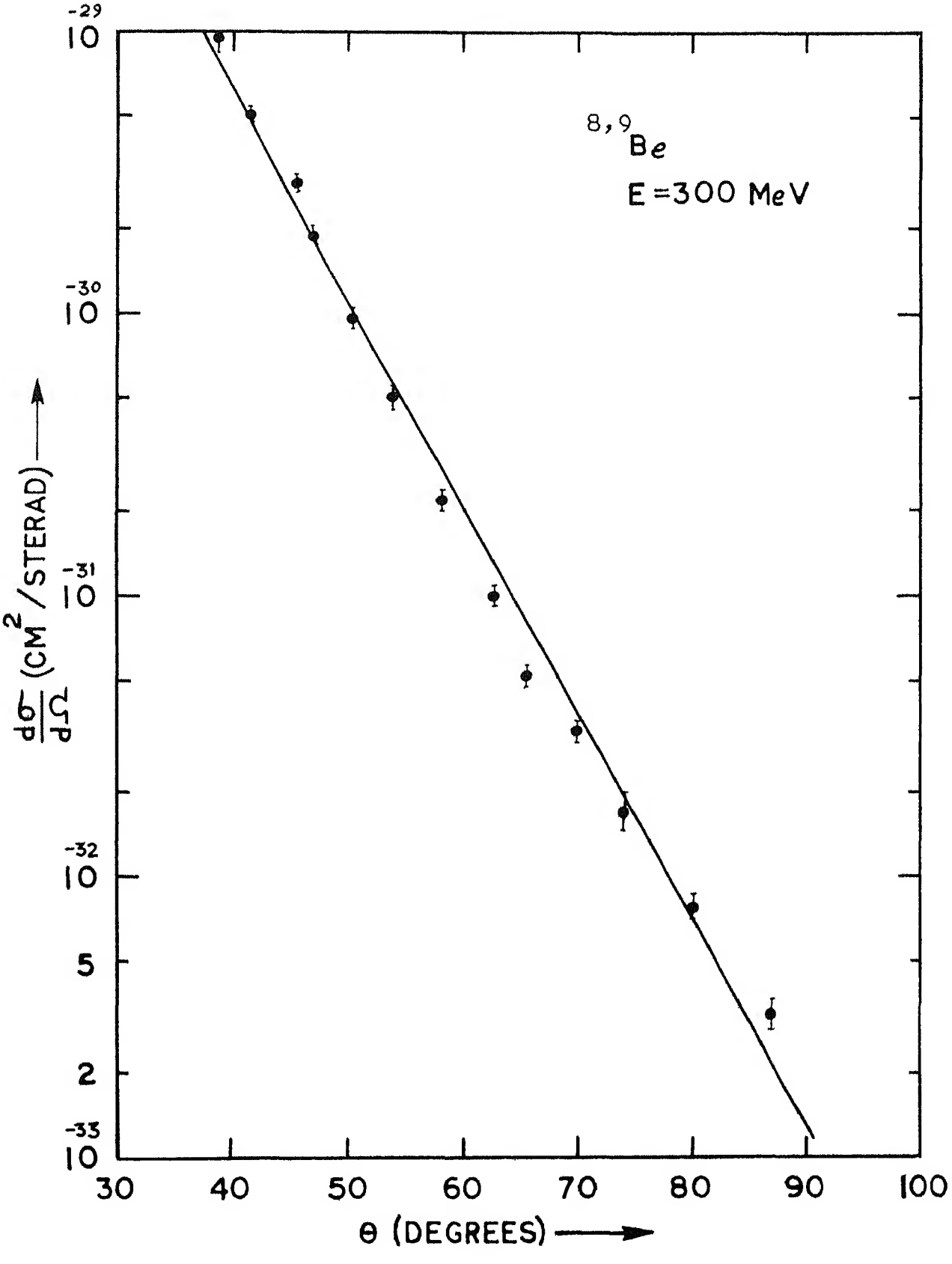

FIG 2 6 Comparison of Hartree-Fock and experimental (ref 22) cross section for ^{8,9} Be at E = 300 MeV

induced in the proton wave functions due to the presence of an additional neutron are negligible

For ^{12}C and ^{16}O nuclei, the HF results at E = 420 MeV along with the experimental points are shown in Figs (2 7) and (2 8) respectively The form factor of ^{12}C nucleus obtained from our calculations along with the results of Ciofi Degli Atti[36] who has included the effects of correlations are shown in Fig (2 9) However, the agreement is somewhat poor For HF results, the diffraction minima are shifted (by about 4^{o} for ^{12}C and 2^{o} for ^{16}O) towards the larger scattering angle It is clear from Table (II 1) that for HF calculations the rms charge radii are somewhat larger and half charge density radii are somewhat smaller than those obtained from electron scattering data using the conventional models The value of the rms radius of ^{16}O is somewhat better than that obtained from Brueckner theory[33]

2.4 Oscillator and Fermi Models for Charge Distribution

As mentioned earlier, the distributions that are most generally used are the oscillator distribution for light nuclei ($A \leq 16$) and the Fermi distribution for medium and heavy nuclei ($A > 16$) In last few years, several attempts[48] have been made to use the Fermi distribution for light nuclei in order to systematize the results on electron scattering for all nuclei The fact that the Fermi distribution could also reproduce the results for light nuclei, it seems that these two models should have some vital features

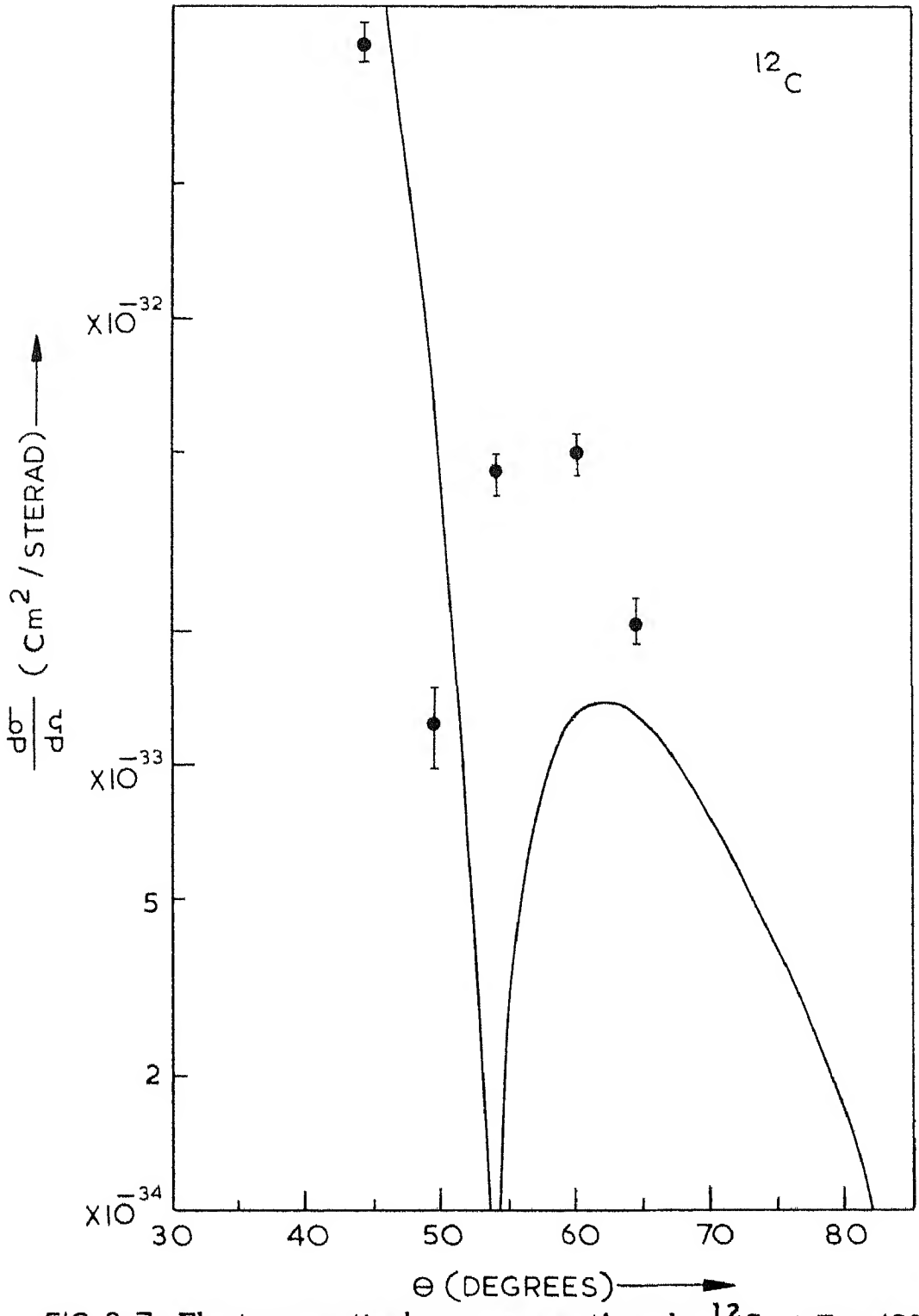

FIG 2 7 Electron scattering cross sections by ^{12}C at E = 420 MeV calculated with the HF charge density Experimental points (ref 19) are shown with errors

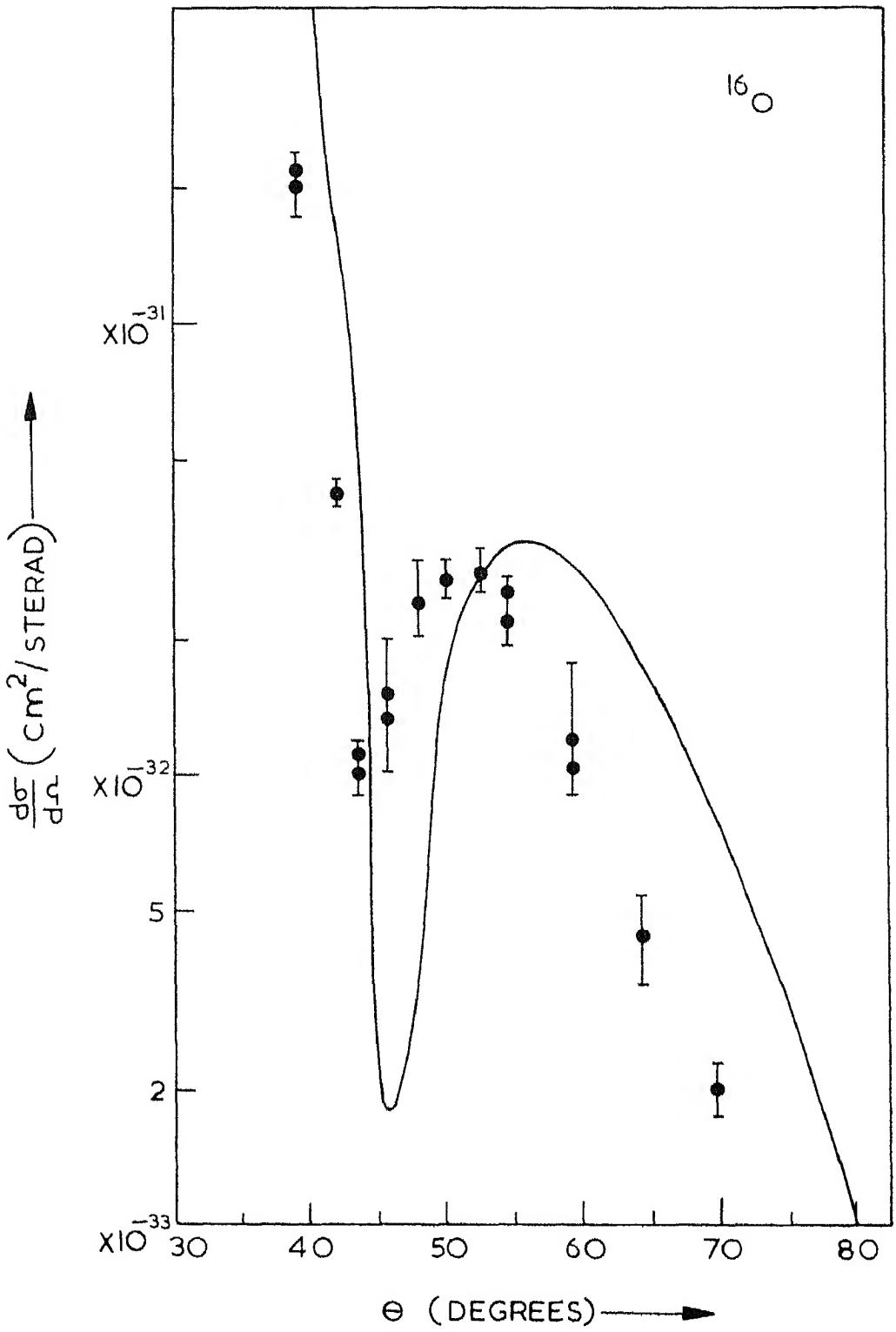

FIG 2 8 **Electron scattering cross section by ^{16}O at E = 420 MeV calculated with the HF charge density Experimental points (ref 19) are shown with errors**

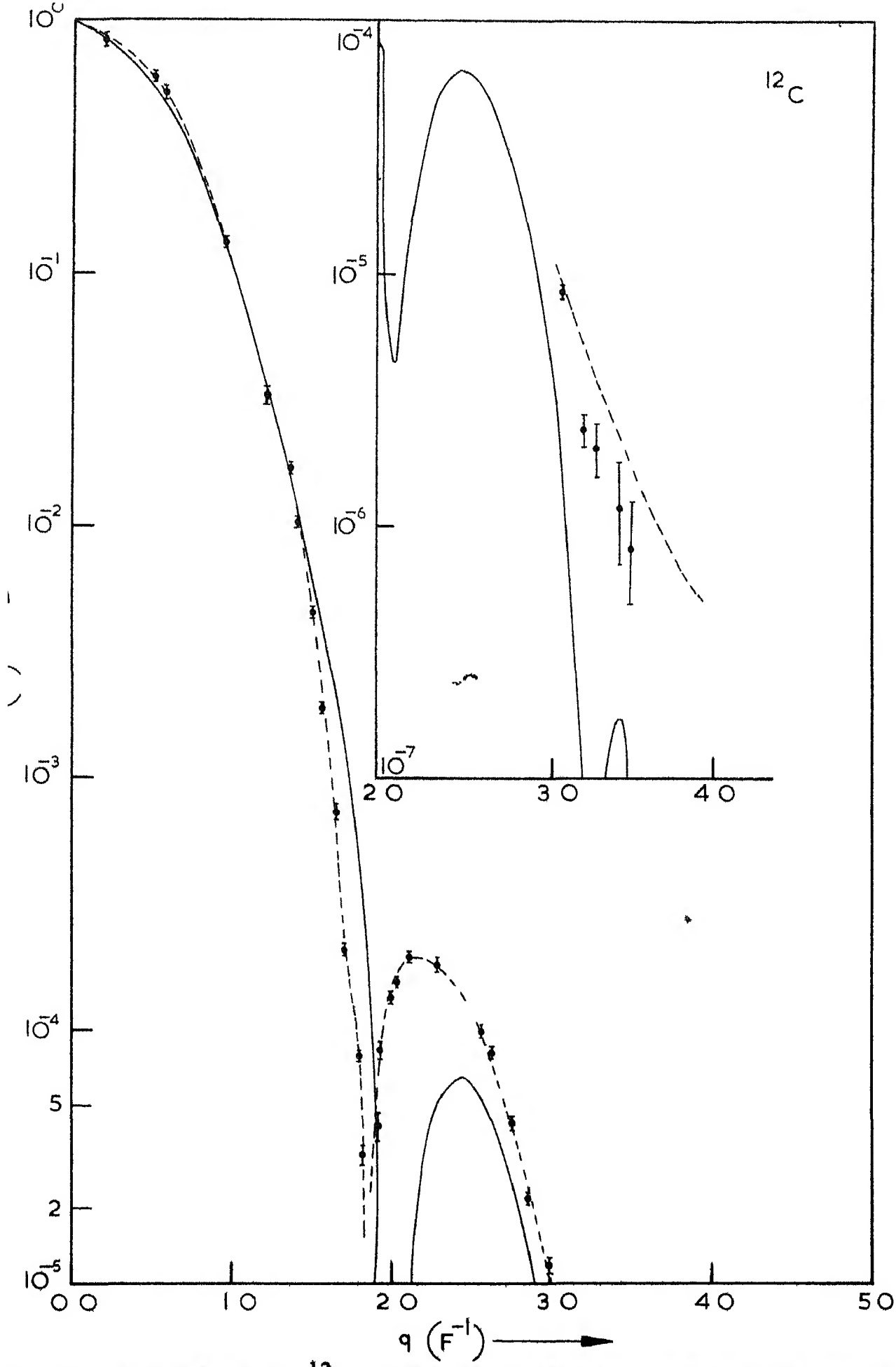

IG 2 9 **Form factor for ^{12}C. The solid curve is calculated with HF results and the dashed curve represents results of Ciofi Degli Atti (ref. 36) obtained**

in common Particularly, as we see below these two models can be correlated in the limit of small momentum transfer In the first part of this section, we derive a general expression for the form factor of a spin zero nucleus in the single particle shell model picture In the later part a relationship between the parameters of these two popular models of nuclear charge distribution is established

2 4a Form Factor for Oscillator Distribution

If we start filling up the single particle shells o_s, op, od, etc with protons, then, for a spin zero nucleus with Z protons the charge density can be written as,

$$\rho(r) = (2\pi Z r^2)^{-1} \left[\sum_{n=0}^{n_{max}} \sum_{\ell_n=0}^{L_n} (2\ell_n+1) R_{n\ell_n}(r)^2 + \right.$$

$$\left. + \tfrac{1}{2} \Delta R_{NL_N}(r)^2 \right] \qquad (2.22)$$

where $$\Delta = Z - 2\sum_{n=0}^{n_{max}} \sum_{\ell_n=0}^{L_n} (2\ell_n+1) = Z - 2\sum_{n=0}^{n_{max}} (L_n+1)^2,$$

$(R_{n\ell_n}(r)/r)$ is the radial part of harmonic oscillator wave fuctions[50], n and ℓ_n are the usual radial and orbital angular momentum quantum nos respectively (N and L_N correspond to the last filling orbit), and L_n is the maximum value which ℓ_n can take for completely filled orbits The factor $2(2\ell_n + 1)$ in (2 22)gives the number of protons in ℓ_n-orbit In practice, as long as the validity of this model is concerned, n does not exceed the value 1 for most of the

nuclei We, therefore, write (2 22) for this simpler case in the form

$$\rho(r) = (2\pi Zr^2)^{-1} \left[\sum_{\ell=0}^{L_0} (2\ell+1)\, R_{0\ell}(r)^2 + \sum_{\ell=0}^{L_1} (2\ell+1) R_{1\ell}(r)^2 + \right.$$

$$\left. + \tfrac{1}{2} \Delta R_{NL_N}(r)^2 \right] \qquad (2\ 23)$$

where N = 0 or 1 (depending upon the last filling orbit), and L_0 and L_1 are the maximum values which ℓ can take for n = o and n = 1 respectively

For the spherically symmetric charge distribution (2 23), the form factor with the help of (2.5) can be written as,

$$F(q) = \frac{2}{Z} \left[\sum_{\ell=0}^{L_0} (2\ell+1)\, I_{0\ell} + \sum_{\ell=0}^{L_1} (2\ell+1)\, I_{1\ell} + \tfrac{1}{2} \Delta\, I_{NL_N} \right] \qquad (2\ 24)$$

where

$$I_{0\ell} = \tfrac{1}{2} N_{0\ell}^2 \Gamma(\ell+3/2)\, b^{2\ell+3}\, {}_1F_1(\ell+3/2,\ 3/2,\ -q^2b^2/4)$$

$$I_{1\ell} = \tfrac{1}{2} N_{1\ell}^2 \Gamma(\ell+3/2)\, b^{2\ell+3} \left[{}_1F_1(\ell+3/2,\ 3/2,\ -q^2b^2/4) + \right.$$

$$+ \frac{(2\ell+5)}{(2\ell+3)}\, {}_1F_1(\ell+7/2,\ 3/2,\ -q^2b^2/4) -$$

$$\left. -2\, {}_1F_1(\ell+5/2,\ 3/2,\ -q^2b^2/4) \right]$$

where ${}_1F_1$ (a, c, z) is the confluent hypergeometric function, $N_{n\ell}$ is the normalization constant of harmonic oscillator fuctions[50] and the oscillator well parameter $b = \sqrt{\hbar/M\omega}$. The formula for solving such integrals is given in Appendix I. For p-shell nuclei the expression (2 24) reduces to a

well known form[19]

$$F(q) = [1-\tfrac{1}{2}\ \alpha q^2 b^2/(2+3\alpha)]\ \exp(-q^2b^2/4) \qquad (2\ 25)$$

where $\alpha = (Z-2)/3$ In general one can choose different oscillator parameters b for each shell in (2 24) For example, the result for d-shell nuclei is

$$F_{d\text{-shell}}(q) = \frac{2}{Z}\,[\exp(-q^2b_s^2/4) + (3-\tfrac{1}{2}\ q^2b_p^2)\ \exp(-q^2b_p^2/4) + \tfrac{1}{2}(Z-8)(1-\tfrac{1}{3}\ q^2b_d^2 + \tfrac{1}{60}\ q^4b_d^4)\ \exp(-q^2b_d^2/4)] \qquad (2\ 26)$$

2 4b The Relation Between Harmonic Oscillator and Fermi Model

The form factor for two parameter Fermi model (under the assumption that the skin thickness is smaller than the half charge density radius) is given by[49]

$$F_F(q) = (4\pi^2\rho_o c a_o/q)\ [(\pi a_o/c)\ \sin(qc)\ \cosh(\pi q a_o)\times \times\ \operatorname{cosech}^2(\pi q a_o) - \cos(qc)\ \operatorname{cosech}(\pi q a_o)] \qquad (2\ 27)$$

In the limit of small q this can be rewritten as,

$$F_F(q) = 4\pi\ \rho_o \sum_{\nu=0}^{\infty} \frac{(-1)^\nu\ a_o^{2\nu+3}}{(2\nu+1)!}\ [\frac{y^{2\nu+3}}{(2\nu+3)} + + \sum_{\mu=1}^{\infty} \frac{2(2^{2\mu-1}-1)}{(2\mu)!}\ B_\mu \pi^{2\mu} D^{2\mu-1} y^{2\nu+2}]\ q^{2\nu} \qquad (2\ 28)$$

where B_μ are the Bernoulli numbers, $D \equiv \frac{\partial}{\partial y}$ is the differential operator, and $y = c/a_o$ The condition that the second term in the bracket be nonvanishing is $(2\nu+3) > 2\mu$ Eqn (2 28)

can be expressed in a series form,

$$F_F(q) = A_0 - A_1 q^2 + A_2 q^4 - A_3 q^6 + \qquad (2\ 29)$$

where A's are functions of c and a_0 First few of these are,

$$A_0 = (4\pi \rho_0 c/3)(\pi^2 a_0^2 + c^2)$$

$$A_1 = (4\pi \rho_0 c/90)\ (7\pi^4 a_0^4 + 10\pi^2 a_0^2 c^2 + 3c^4)$$

$$A_2 = (4\pi \rho_0 c/2520)\ (31\pi^6 a_0^6 + 49\pi^4 a_0^4 c^2 + 21\pi^2 a_0^2 c^4 + 3c^6)$$

$$A_3 = (4\pi \rho_0 c/226800)(381\pi^8 a_0^8 + 620\pi^6 a_0^6 c^2 + 29\pi^4 a_0^4 c^4 + + 60\pi^2 a_0^2 c^6 + 5c^8)$$

Now, we successively assume that $\frac{A_2}{A_0} = \frac{1}{21} (\frac{A_1}{A_0})^2$, $\frac{A_3}{A_0} = \frac{1}{31} \times \times (\frac{A_1}{A_0})^3$, then, the series (2 29) can be expressed immediately in a Gaussian form

$$F_F(q) \underset{q \to \text{small}}{\equiv} F_G(q) = A_0 \exp(-b_1^2 q^2/4) \qquad (2\ 30)$$

where

$$b_1^2 = 4\ A_1/A_0 \qquad (2\ 31)$$

The ratios A_1/A_0, A_2/A_0, . etc. are calculated for ^{4}He and it is found that the error involved in these approximations is $\lesssim$ 10% In fact, the HF charge distribution[51] for ^{4}He is also fitted with a Gaussian form by choosing proper cut-off at the tail and the expression (2 31) is verified for the following set of parameters

$$b_1 = 1\ 42\ F\ ,\ c = 1\ 18\ F,\ a_0 = 0\ 4\ F$$

Now we extend this correspondence between the parameters of these two models for p-shell nuclei From

the analysis of the results of high energy electron scattering, it is now well known[52] that the nucleons of s-orbit move in different oscillator potential than those of p-orbit ($b_p \neq b_s$) By using this fact, the form factor (2 25) for p-shell nuclei can be written as

$$F_{h\ o}(q) = 2(2+3\alpha)^{-1}[\exp(-b_s^2q^2/4) + \\ + \tfrac{1}{2}\alpha(3-\tfrac{1}{2}q^2b_p^2)\ \exp(-b_p^2q^2/4)] \qquad (2\ 32)$$

where b_s and b_p are the oscillator parameters for s- and p-orbits respectively By expressing (2.32) in the form of series expansion (2 29) for small q, and then comparing the coefficients of the two series upto q^4 term, after a simple calculation we obtain the relations

$$b_s^2 = \frac{14\delta \pm 5\sqrt{2\alpha(25\alpha\gamma-7\delta^2+14\gamma)}}{2(25\alpha+14)},\quad b_p^2 = \frac{5\alpha\delta \pm \sqrt{2\alpha(25\alpha\gamma-7\delta^2+14\gamma)}}{\alpha(25\alpha+14)} \qquad (2\ 33)$$

where $\delta = 4\ Z\ A_1/A_0$, and $\gamma = 32\ Z\ A_2/A_0$ If one assumes $b_s = b_p = b_2$ and uses α as a parameter+, then the relationship between the parameters of two models becomes

$$b_2^2 = [\delta \pm \sqrt{\delta^2-\gamma Z}]/Z\ ,\quad \alpha = \frac{2\sqrt{\delta^2-\gamma Z}\ (5\sqrt{\delta^2-\gamma Z}\pm 2\delta)}{(25\gamma Z-21\delta^2)} \qquad (2\ 34)$$

It must be noted here that the error involved in getting (2 33) and (2 34) is much less than that involved in

---

+ The choice of α as a parameter, as it is assumed by some authors (ref 22) is arbitrary In that case, the error involved in approximating (2 32) in the form of (2 29) for small q, is reduced

getting (2 31) Because, in order to calculate the two parameters of (2.32), we have equated the coefficients only upto q^4-terms in (2 29) for small q and error arises from q^6 and higher power terms in (2 29) only For ^{12}C nucleus, the relation (2 34) is checked for the following set of parameters given in reference[22]

$$b_s = b_p = 1\ 637\ F\ ,\ a_0 = 0\ 5\ F\ ,\ c = 2\ 24\ F$$

If we assume $b_p > b_s$ then, the relation (2 33) predicts $b_s = 1\ 312$ F, $b_p = 1\ 832$ F for ^{12}C nucleus (in fact we obtain two values for each b_s^2 , b_p^2, b_2^2 and α However, it is reasonable to assume that $b_2^2 > 0$, $\alpha > 0$ and $b_p > b_s$) The form factors for the two models, calculated with the above set of parameters for ^{12}C are shown in Fig (2 10)

Thus, we see that the larger the number of parameters in $F_{h\ o}(q)$, the lesser will be the error involved in extracting these parameters from (2 29). The number of the parameters in $F_{h\ o}(q)$ can be increased further by writing it for a heavier nucleus and choosing different oscillator parameters for each shell In other words, for heavy nuclei (no matter whether q is small or large) $F_{h\ o}(q)$ becomes $F_F(q)$ This justifies the validity of the Fermi distribution for heavy nuclei

The recent results of Frosch et al[25] show that the oscillator distribution does not provide satisfactory agreement with experimental results for ^4He at large values of momentum transfer Our calculations with two-parameter Fermi distribution show that one can still obtain the observed

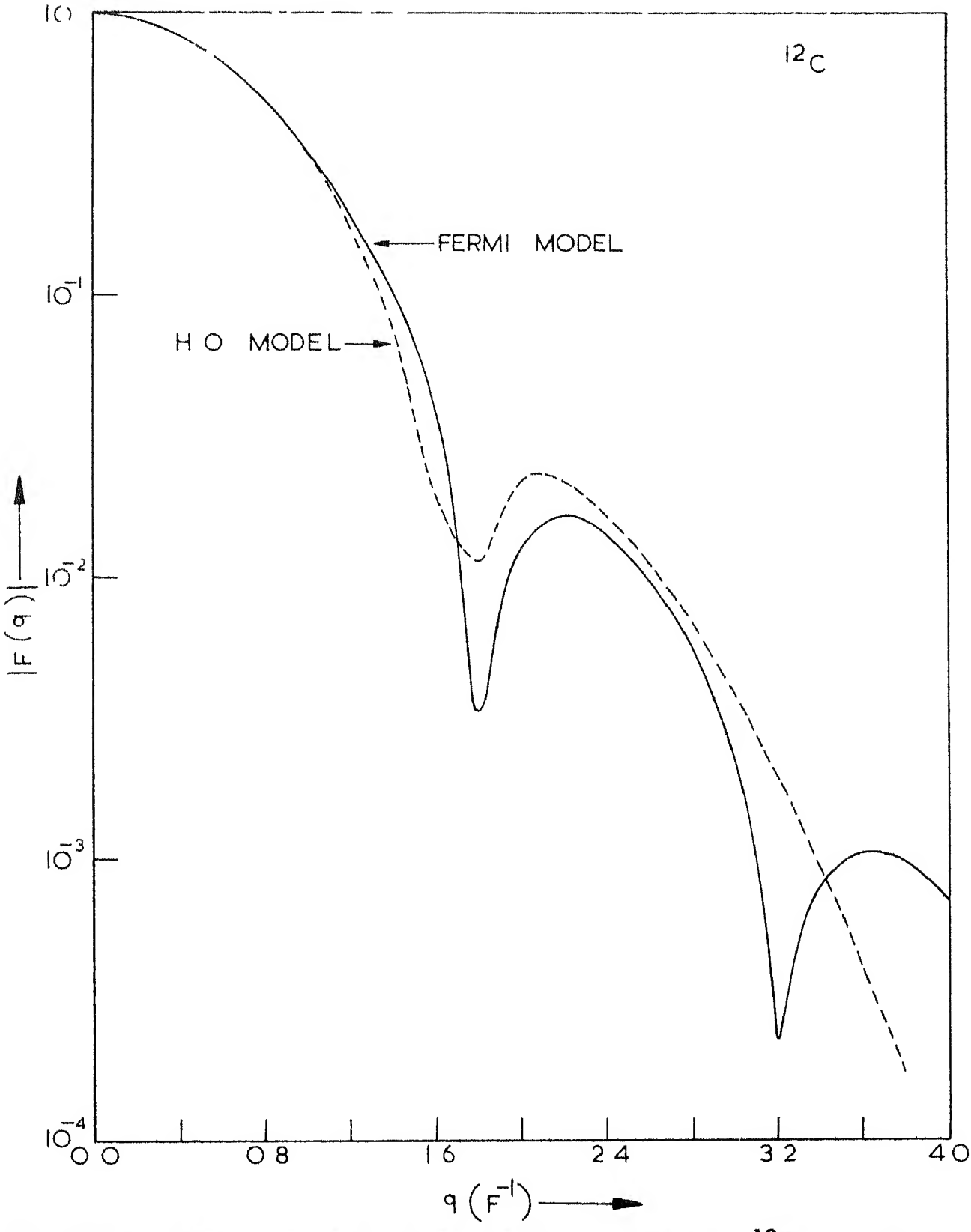

FIG 2 10 **Equivalence of the Fermi and oscillator models for ^{12}C in the limit of small momentum transfer**

2 5a A Model for ^4He

As mentioned in the last section, for large q the oscillator distribution can also be used by increasing the number of parameters. Recently, the calculations are done by Chou[53] by choosing the difference of two Gaussian forms and hence by increasing the number of parameters in the oscillator distribution Here we shall use a distribution of the form

$$\rho(r) = \rho_0(r) + \varepsilon r \, (d/dr) \, \rho_0(r) \qquad (2\ 35)$$

where $\rho_0(r) = \rho_0 \exp(-r^2/b_1^2)$, the usual Gaussian distribution and ε is a parameter The choice of this distribution is based on the criterian that for ^4He being a spin zero nucleus, at large momentum transfers the second term would provide a density fluctuation[46]

Now, for $\rho_0(r)$ as a Gaussian form, after proper normalization (2.35) becomes,

$$\rho(r) = \pi^{-3/2} b_1^{-3} (1-3\varepsilon)^{-1} (1-2\varepsilon r^2/b_1^2) \exp(-r^2/b_1^2) \qquad (2\ 36)$$

which is similar to the distribution of p-shell nuclei (see eqn (2.21)) with negative α Thus, the introduction of second term in (2 35) increases the constant central part of charge density (cf. Fig (2 11)), which is observed by Frosch et al[25] The form factor and rms radius corresponding to (2 36) are given by

$$F(q) = \left[1 + \frac{\varepsilon q^2 b_1^2}{2(1-3\varepsilon)}\right] e^{-b_1^2 q^2/4}, \quad \sqrt{\langle r^2 \rangle} = b_1 \left[\frac{3(1-5\varepsilon)}{2(1-3\varepsilon)}\right]^{\frac{1}{2}} \qquad (2\ 37)$$

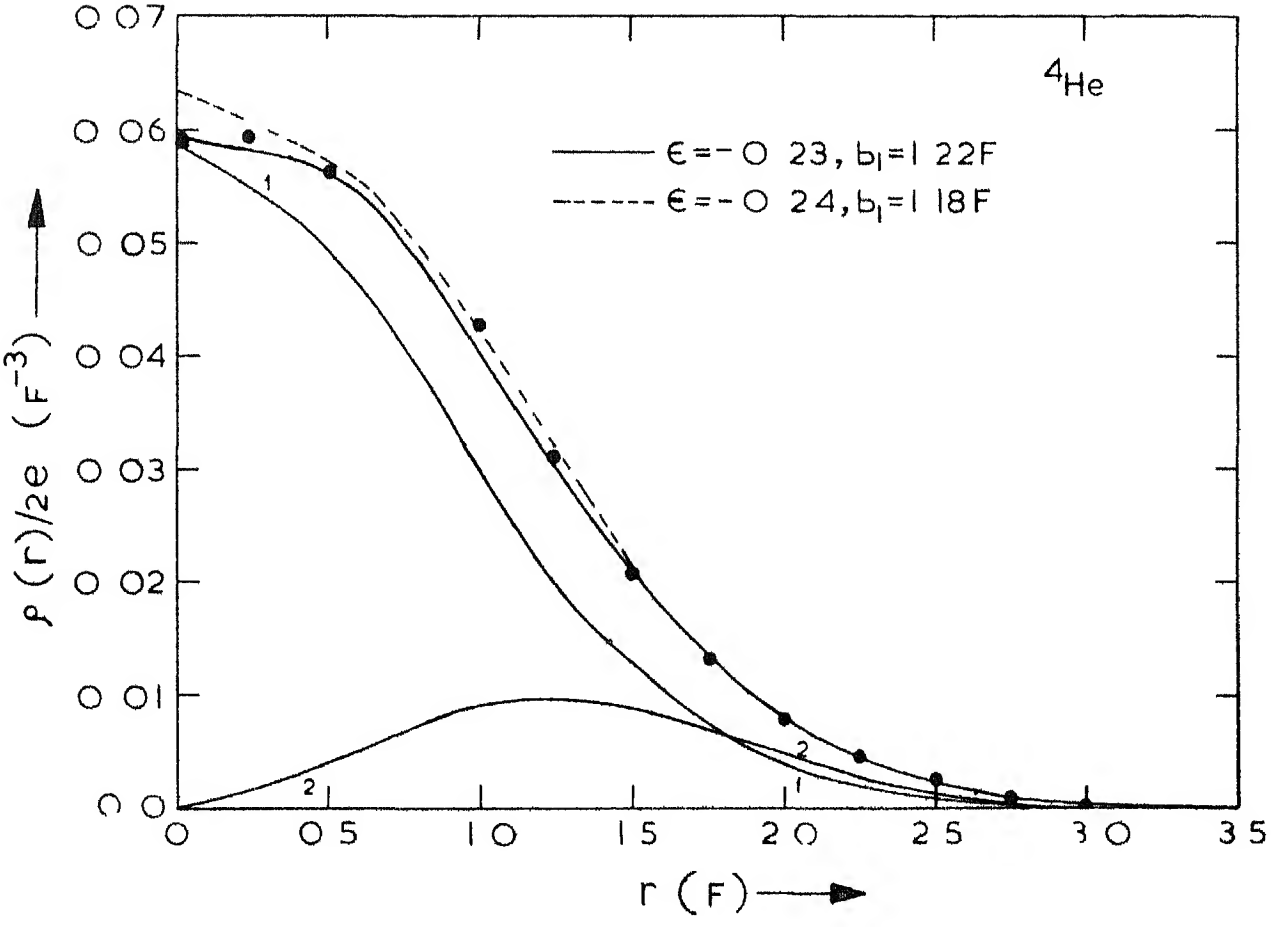

FIG 2 11 Charge density for ^{4}He obtained for the simple model (eqn (2 35)) for two sets of parameters Curves denoted by 1 and 2 are corresponding to the first and the second terms of eqn (2 35) for $\epsilon = -0\ 23$, $b_1 = 1\ 22$ F Experimental points are from Frosch et al (ref 25)

The results obtained for this model are shown in Figs (2 11) and (2 12) along with the experimental points The results are obtained for two sets of parameters given in Table (II 2) The form factor, as it is clear from Fig (2 12), agrees fairly well for small values of momentum transfer ($q^2 < 10\ F^{-2}$) However, the agreement is somewhat poor for large values of q^2 For the sake of comparison the results obtained by Jain[35] with Irving wave functions[54] and velocity-dependent potential, and by other authors are given in Table (II 2) Our result are in somewhat better agreement with experiments than Jain's results In particular, the results corresponding to $\varepsilon = -0\ 23$, $b_1 = 1\ 22\ F$ are in fairly good agreement with experiments For this case the contribution from each term of (2 35) is shown in Fig (2 11)

2 5b Jastrow Method Comparison with HF Results

In the Jastrow method[38] one writes the correlated nuclear charge density in the form

$$\rho(\vec{r}_1,\vec{r}_2, \quad ,\vec{r}_A) = |\Phi(\vec{r}_1,\vec{r}_2, \quad ,\vec{r}_A)|^2 \prod_{i<j}^{A} [1-f(r_{ij})] \qquad (2\ 38)$$

where A is the number of nucleons in the nucleus, Φ is the uncorrelated ground state wave function (shell model wave function) The function $f(r_{ij})$ introduces correlation of the (i,j) pair of nucleons at small distances $r_{ij} = |\vec{r}_i - \vec{r}_j|$ and satisfies the boundary conditions

$$f(r_{ij}) \to 0, \text{ for } r_{ij} \to \infty, \quad f(r_{ij}) \to 1, \text{ for } r_{ij} \to 0$$

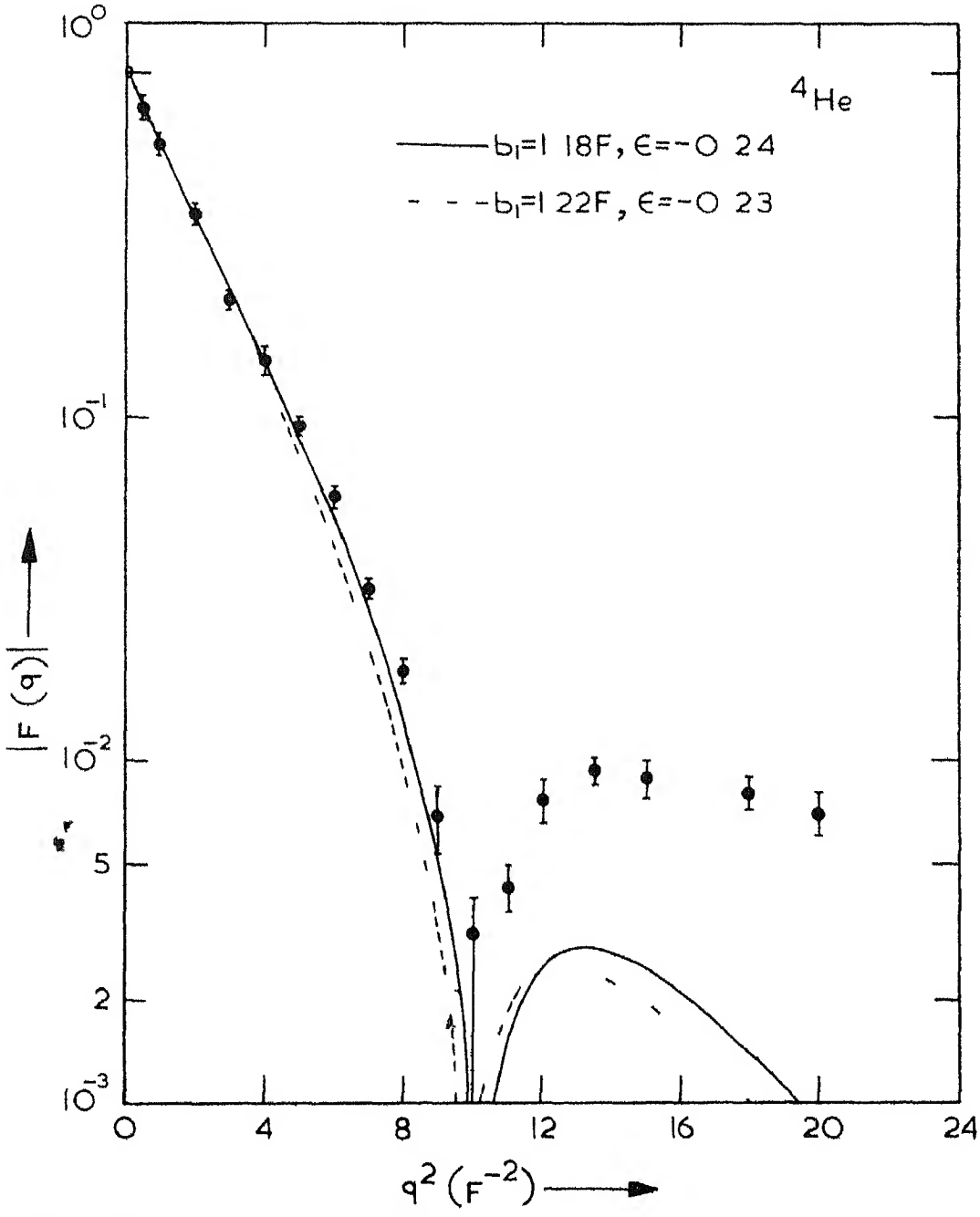

FIG 2 12 Form factor for ^{4}He obtained for the simple model (Eqn (2 35)) for two sets of parameters Experimental points of Frosch et al (ref 25) are shown with errors

TABLE II 2

Comparison of the results for ^{4}He obtained from the present calculations with those of other authors

Various methods	Ref	$\sqrt{\langle r^2 \rangle}$ (F)	c(F)	t(F)	$\rho_{ch}(o)/2e$
Present calculations(HF results)	-	1 778	1 18	1 76	0 0636
Present calculations (A simple model ε= -0 23, b_1 = 1 22 F)	-	1 684	1 28	1 45	0 0587
Present calculations (A simple model ε = -0 24, b_1 = 1 18 F)	-	1 635	1 26	1 60	0 063
Irving wave functions	35)	1 73	1 08	1 58	0 0767
Hard -core[a] (r_c = 0 5 F)	34)	1 67	1 13	1 55	0 076
Hard -core[a] (r_c = 0 6 F)	34)	1 73	1 20	1 56	0 065
Gaussian model	18)	1 68	1 14	1 64	0 0698
Experimental	25)	1 67	1 32	1 45	0 0595

a Tang and Herndon

when we expand the product in (2 38) we get

$$\rho(\vec{r}_1, \quad ,\vec{r}_A) = |\Phi(\vec{r}_1, \quad ,\vec{r}_A)|^2 [1-\sum_{i<j} f(r_{ij}) + \sum_{i<j}\sum_{j<k} f(r_{ij})f(r_{jk})- \quad] \qquad (2\ 39)$$

various terms in this series are corresponding to the contributions of different number of correlated pairs (no correlated pairs, one correlated pair, two correlated pairs etc) For electron scattering, we usually retain the series corresponding to the one correlated pair term and the forms of $f(r_{ij})$ chosen very often are,

$$f(r_{ij}) = e^{-\beta r_{ij}^2}, \quad f(r_{ij}) = e^{-\beta[(r_{ij}/r_c)^2-1]}$$

which are corresponding to the repulsive soft and repulsive hard cores between nucleon-nucleon forces respectively The quantities β (the so called 'correlation parameter') and r_c (correlation length) are determined by fitting the experimental results

Using the Jastrow method, the form factor of ^{4}He is calculated by several authors[34,35] The methods of these authors differ either in the choice of various correlation fuctions of in the choice of including antisymmetrization of the wave function of alpha-particle. Some of these results are compared with the HF calculations in Fig (2 4) Overall comparison shows that the HF results are in better agreement with experiments than those obtained by Tang and Herndon[34] and Czyz and Lesniak[34] However, a little discrepancy arises

in the region of diffraction minimum The results of Czyz and Lesniak show the diffraction minimum at $q^2 = 10\ 8F^{-2}$ while HF results show at $q^2 = 11F^{-2}$ against the experimental result at $q^2 = 10F^{-2}$

The calculations, after including the Jastrow correlation as well as the effects of antisymmetrization in the nuclear wave function are also done by Ciofi Degli Atti[36] for ^{12}C nucleus He has made explicit calculations for the correlated part of the form factor in the shell model scheme However, he could not get better agreement for $q > 3F^{-1}$ (see Fig (2 9)) He has further extended[37] his calculations for ^{6}Li The effects of Jastrow type correlation in ^{16}O charge density have not yet been studied

Another way of introducing correlations in the nuclear density is the following

$$\rho(\vec{r}_1, \quad ,\vec{r}_A) = |\Phi(\vec{r}_1, \quad ,\vec{r}_A)|^2 \left[\prod_{i<j}^{A} (1-f(r_{ij}))\right]^2 \tag{2 40}$$

Now, if we expand further the square of the product in the right hand side, it reduces to a similar series as (2 39) Up to one pair term, this gives identical results as obtained previsouly from (2 38) except a slight modification for the correlation parameter β The difference between these two ways may arise when one includes the contribution of many pair terms in the series

2 6 Comments and Discussion of the Results

For the large values of momentum transfer q, the results of elastic electron scattering are fairly well explained by introducing the short range dynamical correlations in the nuclear charge distribution The Jastrow method, a usual way of introducing the correlations, seems to be the special case of general unitary transformation approach discussed in section (2 2) Though, the HF calculations are somewhat difficult for heavier nuclei, they have several advantages over the Jastrow method Firstly, there is no correlation parameter to fit with the experiments Secondly, the problem of orthonormality of the correlated wave functions, which complicates the calculations does not arise We expand the correlated wave functions in terms of harmonic oscillator basis (cf eqn (2 16)) The determination of the expansion coefficients c's in a self consistent manner is the main criteria to justify the significance of the present HF method

As mentioned in section (2.3) (particularly for ^{12}C and ^{16}O) though the agreement between HF results and the experimental values is not excellent, these calculations provide fairly good binding energies[40-42] Besides, it is clear from Figs (2 4), (2 7) and (2 8) that the HF results show a little shift, $1F^{-2}$ (about 6^{o} at E = 420 MeV) for ^{4}He 4^{o} for ^{12}C and 2^{o} for ^{16}O, of diffraction minimum towards the larger angle side A similar shift of diffraction minimum is also expected in case of the predicted results of ^{8}Be HF

results also show a shift of shoulder of the curve towards the large scattering angle. In this region, the agreement with experiments is somewhat poor. These discrepancies are not surprising. The wave functions used here to calculate the charge density are obtained for spherical Hartree-Fock. In this case the correlated wave function is expanded in terms of harmonic oscillator basis and the summation is restricted over only radial quantum number n (cf. eqn. (2.16)). However, different unoccupied ℓ-orbitals may also contribute and consequently improve the results. In other words, the skin part of the charge distribution is not properly treated in these calculations. Nuclear structure calculations with ℓ-mixing for ^{12}C have recently been done by Pal and Stamp[55]. However, they have not calculated the charge distribution. The HF calculations for medium weight nuclei using the same technique and Yale potential matrix elements are done by Gunye[56]. The charge distributions obtained by Gunye for medium mass nuclei are in fair agreement with the electron-scattering results.

In Brueckner's K-matrix theory the two-body non-local correlation is relatively stronger near the centre of the nucleus and its state dependence causes to pull the wave functions in. That is why, the charge is mostly accumulated near the centre of the nucleus (cf. Fig. (2.3)). On the other hand, no extra non-local character of the interaction is used in the present calculations except that, a part which is automatically included in the HF method due to the

antisymmetry of the wave functions It shows that the non-local nature of the nuclear forces is not as stronger as in Brueckner theory

In section (2 4) we have established the relationship between the parameters of two important models namely, the harmonic oscillator and Fermi distributions However, this relationship is still restricted for small values of q By increasing the number of parameters in a definite way, the use of oscillator distribution at large values of q is justified One immediate example is the use of correlation parameter β in the oscillator charge density For large values of q and for closed p-shell nuclei, the failure of the usual oscillator distribution is of immediate prediction on the basis of the results obtained in section (2 4) For example, the constantly improving experimental techniques should make it possible to observe other diffraction minima in the form factor of ^{12}C (cf Fig (2 10)) at large q Mathematically, it is obvious that $F_{h\ o}(q)$ in the form of (2 32) will not be able to explain them However, Fermi distribution will be helpful, because of the occurring periodic functions in the expression of $F_F(q)$

Finally, mention should be made of the success of a simple model, described in section (2 5), for ^4He This simple model gives somewhat better results compared to the results obtained by Jain[35] (cf Table (II 2)) using Irving[54] wave functions By comparing Figs (2 4) and (2 12) it can be easily seen that the overall behaviour of the form factor